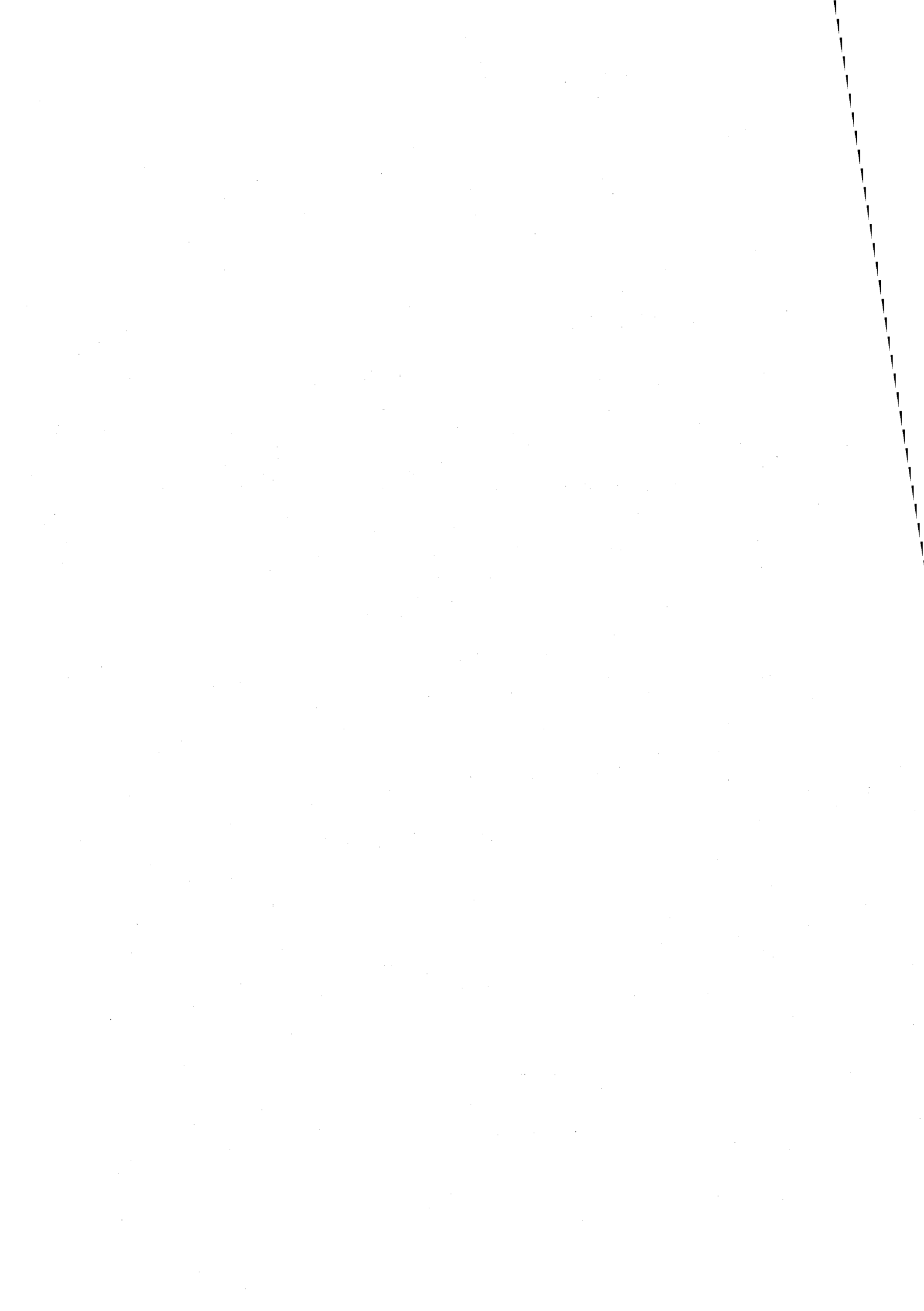


# **English Abstracts**



## **2S01 : Synthesis and properties of external-stimuli responsive complexes**

Nishihara, H. (Univ. of Tokyo)

Intelligent molecules, the structures and properties of which are facilely and reversibly changeable by application of external physical and chemical stimuli, have attracted much recent attention relative to the development of new molecule-based devices. In this paper, recent advances in two types of such d-p interaction systems responding to external stimuli are presented. The first type involves donor (D)-acceptor (A) conjugated molecules comprising a ferrocene and a proton-responsive quinonoid compound. The protonation to carbonyl groups of the anthraquinone moiety in 1-ferrocenylethynylanthraquinone causes intramolecular electron transfer leading to a novel structural change into a diamagnetic  $\eta^6$ -fulvene Fe(II) complex, of which Mössbauer spectra has indicated an occurrence of temperature-dependent reversible valence tautomerization with a paramagnetic ferrocenium (Fe(III)) complex. The formation of such valence tautomers and their properties depend significantly on the number of D and A groups, the D/A ratio, and the substitution position of D on anthraquinone (A). The second type of d- $\pi$  interaction systems involves redox-active metal complexes conjugated with the isomerizable azo group. A new reversible isomerization cycle for 4-ferrocenylazobenzene accomplished by combination of a single green light (546 nm) and redox change between Fe(II) and Fe(III) was discovered. In the Fe(II) state, trans-to-cis isomerization proceeded upon the green light irradiation exciting the metal-to-ligand charge transfer (MLCT), the oxidation to the Fe(III) state followed by irradiation with the same green light led to the cis-to-trans back-reaction to recover almost all of the trans-form. The "on-off switching" of the MLCT character played an important role in the redox-dependent response to the green light for the isomerization.

## **2S02 : Moessbauer Exploration of the Surface of Mars with MIMOS II and the Mars-Exploration-Rovers**

Klingelhoefer, G (Mainz Univ.)

## **2S03 : Chemical studies of the transactinide element, rutherfordium (Rf), at JAERI**

Nagame, Y. (Japan Atomic Energy Research Institute)

Chemical studies of element 104, rutherfordium (Rf), at JAERI (Japan Atomic Energy Research Institute) are reviewed. To perform chemical experiments of transactinide elements ( $Z=104$ ) with single atoms on an atom-at-a-time scale, we have developed some experimental apparatuses: a beam-line safety system for the usage of a

gas-jet coupled radioactive target and recoil chamber, a rotating wheel catcher apparatus for the measurement of  $\alpha$  and spontaneous fission (SF) decay of transactinides, and an automated rapid ion-exchange separation apparatus based on high performance liquid chromatography coupled with an on-line  $\alpha$ -particle detection system. The transactinide nuclide, 78-s  $^{261}\text{Rf}$  has been successfully produced through the reaction of  $^{248}\text{Cm}(^{18}\text{O},5\text{n})$  at the JAERI tandem accelerator. The evaluated production cross section is about 10 nb, indicating that the production rate is approximately 2 atoms per min. On-line anion-exchange experiments of Rf together with the group-4 elements, Zr and Hf, in acidic solutions have been conducted with the developed ion-exchange separation system. From the systematic study of the chemical properties of Rf, it has been found that the chemical behavior of Rf is quite similar to that of the group-4 elements Zr and Hf; the results definitely indicate that Rf is the member of the group-4 elements. However, we have observed unexpected chemical behavior of Rf recently; the fluoride complex formation of Rf is quite different from those of the homologues Zr and Hf. In this report, characteristic ion-exchange behavior of Rf studied at JAERI is discussed.

## **2S04 : A study on the complexation and sorption of actinides and lanthanides in environment**

Takahashi, Y. (Department of Earth and Planetary Systems Science, Graduate School of Science, Hiroshima University)

## **1A01 : Reversed-phase extraction chromatography of Zr and Hf in the TBP/HCl system -Model experiments for chemical characterization of element 104, rutherfordium-**

Haba, H.,<sup>a</sup> Tsukada, K.,<sup>b</sup> Akiyama, K.,<sup>b</sup> Asai, M.,<sup>b</sup> Toyoshima, A.,<sup>b,c</sup> Ishii, Y.,<sup>b,d</sup> Enomoto, S.,<sup>a</sup> Nagame, Y.<sup>b</sup> (<sup>a</sup>Cyclotron Center, RIKEN, <sup>b</sup>Advanced Sci. Res. Center, JAERI, <sup>c</sup>Graduate School of Sci., Osaka Univ., <sup>d</sup>Graduate School of Sci. and Engineering, Shizuoka Univ.)

We plan to investigate extraction behavior of element 104, rutherfordium (Rf), in the TBP/HCl system together with its lighter homologues Zr and Hf. The distribution coefficients ( $K_d$ ) of Zr and Hf on the TBP resin for a reversed-phase extraction chromatography were measured in 6–12 M HCl with the batch method using the radiotracers  $^{89}\text{Zr}$  and  $^{175}\text{Hf}$ . It was found that the  $K_d$  values of Zr and Hf increase steeply with an increase of HCl concentration, [HCl], and that the separation factor  $K_d(\text{Zr})/K_d(\text{Hf})$  is high at 7 M (~10) and decrease with [HCl], indicating that the stability of chloride complexes of Zr is stronger than that of Hf. In the near future, we will conduct a TBP-extraction experiment of  $^{261}\text{Rf}$  in 7 M HCl using the Automated Ion exchange separation apparatus coupled with the Detection system for Alpha spectroscopy (AIDA).

## **1A02 : Formation of anionic fluoride complex of rutherfordium (Rf); Anion-exchange behavior of hydrofluoric acid / nitric acid mixed solution system**

Toyoshima, A.,<sup>a,b</sup> Tsukada, K.,<sup>b</sup> Asai, M.,<sup>b</sup> Haba, H.,<sup>c</sup> Akiyama, K.,<sup>b</sup> Ishii, Y.,<sup>b,d</sup> Nishinaka, I.,<sup>b</sup> Sato, T.,<sup>b</sup> Hirata, M.,<sup>b</sup> Nagame, Y.,<sup>b</sup> Sato, W.,<sup>a</sup> Matsuo, K.,<sup>a</sup> Tani, Y.,<sup>a</sup> Saika, D.,<sup>a</sup> Kitamoto, Y.,<sup>a</sup> Hasegawa, H.,<sup>a</sup> Shinohara, A.,<sup>a</sup> Goto, S.,<sup>c</sup> Ito, M.,<sup>c</sup> Saito, J.,<sup>c</sup> Kudo, H.,<sup>c</sup> Sakama, M.,<sup>f</sup> Yokoyama, A.,<sup>g</sup> Morishita, K.,<sup>h</sup> Sueki, K.,<sup>i</sup> Nakahara, H.,<sup>b</sup> Schädel, M.<sup>j</sup> (<sup>a</sup>Graduate School of Sci., Osaka Univ., <sup>b</sup>Advanced Sci. Res. Center, JAERI, <sup>c</sup>Cyclotron Center, RIKEN, <sup>d</sup>Graduate School of Sci. and Engineering, Sizuoka Univ., <sup>e</sup>Faculty. of Sci., Niigata Univ., <sup>f</sup>Dep. of Chemistry, Radiologic Sci. and Engineering, Univ. of Tokushima, <sup>g</sup>Graduate School Nat. Sci. Tech., Kanazawa Univ., <sup>h</sup>Faculty of Sci., Kanazawa Univ., <sup>i</sup>Dep. of Chemistry, Univ. of Tsukuba, <sup>j</sup>GSI)

The formation of the anionic fluoride complex of rutherfordium (Rf) was studied by an anion-exchange method in hydrofluoric acid / nitric acid mixed solution system on an atom-at-a-time basis. It was clearly found that the adsorption behavior of Rf is quite different from the lighter homologues, Zr and Hf, and was suggested that the hexafluoride complex  $\text{RfF}_6^{2-}$  is formed in two orders of magnitude higher concentration of the fluoride ion than  $\text{ZrF}_6^{2-}$  and  $\text{HfF}_6^{2-}$ .

## **1A03 : Anion-Exchange Chromatographic Behavior Of Rutherfordium (Rf) In Hydrofluoric Acid**

Tsukada, K.,<sup>a</sup> Toyoshima, A.,<sup>a,b</sup> Haba, H.,<sup>c</sup> Asai, M.,<sup>a</sup> Akiyama, K.,<sup>a</sup> Nishinaka, I.,<sup>a</sup> Nagame, Y.,<sup>a</sup> Saika, D.,<sup>b</sup> Matsuo, K.,<sup>b</sup> Sato, W.,<sup>b</sup> Shinohara, A.,<sup>b</sup> Ishizu, A.,<sup>d</sup> Ito, M.,<sup>d</sup> Saito, J.,<sup>d</sup> Goto, S.,<sup>d</sup> Kudo, H.,<sup>d</sup> Kikunaga, H.,<sup>c</sup> Kinoshita, N.,<sup>c</sup> Kato, C.,<sup>c</sup> Yokoyama, A.,<sup>c</sup> Sueki, K.,<sup>j</sup> (<sup>a</sup>Advanced Sci. Res. Center, JAERI, <sup>b</sup>Graduate School of Sci., Osaka Univ., <sup>c</sup>Cyclotron Center, RIKEN, <sup>d</sup>Faculty. of Sci., Niigata Univ., <sup>e</sup>Graduate School Nat. Sci. Tech., Kanazawa Univ., <sup>f</sup>Dep. of Chemistry, Univ. of Tsukuba)

The  $K_d$  value of Rf was directly measured from its elution curve on the anion-exchange chromatography with 5.4 M HF solution by using the modified AIDA. The anion-exchange experiments were performed 511 times and about 50  $\alpha$ -events of 78-s  $^{261}\text{Rf}$  and its daughter 25-s  $^{257}\text{No}$  were registered in the energy range of 8.0-8.3 MeV in the fractions. The peak volume of the elution curve of  $^{261}\text{Rf}$  was observed around 200  $\mu\text{L}$ . The  $K_d$  value of Rf was evaluated to be 20-40 mL/g.

## **1A04 : Effective Fusion Barrier in Entrance Channel for Cold Fusion Reaction Leading to SHE Production**

Ichikawa, T.,<sup>a</sup> Iwamoto, A.,<sup>b</sup> Moller, P.,<sup>c</sup> Sierk, A.<sup>c</sup> (<sup>a</sup>JAERI ASR, <sup>b</sup>JAERI, <sup>c</sup>LANL)

We calculate effective fusion barriers in the entrance channel in cold fusion reactions with a model where projectile deformation and zero-point vibration are taken into account. In the entrance channel, the potential energy of the system consists of the sum of the interaction energy between the target and projectile and the self energy for projectile deformations. The interaction energy is calculated on the basis of the Finite Range Liquid Drop Model (FRLDM) and the self energy of projectiles is calculated by taking account of the shell correction energy. The effective fusion barrier is defined as the energy where the instability occurs due to the vanishing of the zero-point energy level in the potential energy surface. The zero-point energy is calculated with the WKB approximation. Except for the system where projectile has a strong shell effect, it seems that our results are consistent with the experimental data. From the comparison with the spherical barrier, we discuss the importance of the deformation and zero-point vibration in the entrance channel in heavy-ion reactions.

## **1A05 : Development of rapid transport system and rapid preparation method for $\alpha$ -emitting source**

Manabe, K.,<sup>a</sup> Takamiya, K.,<sup>b</sup> Shibata, S.<sup>b</sup> (<sup>a</sup>Graduate School of Engineering, Kyoto Univ., <sup>b</sup>Res. Reactor Inst., Kyoto Univ.)

We have developed a transport system for recoiled atoms using dry ice powder and rapid preparation method for  $\alpha$ -emitting source.

The transporting efficiency of this system was measured using FP from  $^{252}\text{Cf}(\text{sf})$ . The  $\text{CO}_2$  siphon cylinder, the  $^{252}\text{Cf}$  source chamber, and the collection chamber were connected by Teflon tubes. FP caught by dry ice powder were transported with  $\text{CO}_2$  gas to the collection chamber. In the case of transporting FP in short distance, the transporting efficiency was measured to be 41%. For transporting FP longer distance with higher efficiency, the transport system has been optimized.

The rapid preparation method for  $\alpha$ -emitting source using coprecipitation method has also been developed. For the purpose of rapid preparation of the source by means of coprecipitation, the following method was examined. At first, a precipitation of  $\text{La}(\text{OH})_3$  was prepared and filtered. Secondly, the tracer solution containing the target nuclides and precipitation reagent were mixed. Finally, this mixture was poured on the filter paper containing the carrier precipitation. It was found that this method enables the rapid preparation of  $\alpha$ -source uniformly.

## **1A06 : KENS Experiment 1: Measurement of spatial distribution of neutrons in concrete shield by activation detectors and IP technique**

Masumoto, K., Wang, Q.B., Toyoda, A., Matsumura, H., Nakao, N., Takahashi, K., Kawai, M. (KEK)

The high-energy neutron irradiation facility was constructed in the KENS experimental room for the neutron penetration and activation experiment. To check neutron profile, many gold and aluminum foils were set inside and outside of concrete shield to measure the reaction rate of  $^{197}\text{Au}(\text{n},\gamma)^{198}\text{Au}$ ,  $^{27}\text{Al}(\text{n},\alpha)^{24}\text{Na}$  and  $^{27}\text{Al}(\text{n},\text{o}2\text{n})^{22}\text{Na}$ . Induced radioactivities of activation detectors were simultaneously measured by the IP technique. Specific activities of several detectors were also measured by Ge-detector to convert from PSL values to reaction rates of each foil. The attenuation behaviors of three kinds of neutron reactions were similar to each other. It means neutron spectra of low energy part (< several MeV) were almost constant inside the shield. The ratio of thermal to epithermal reaction was constant inside the shield and its cadmium ratio was 2. It was confirmed that the MARS14 code calculation could reproduce these experimental results very well. As the IP technique is sensitive accurate and simple for relative radioactivity measurement, this method is very suitable for the measurement of spatial distribution of neutrons.

#### **1A07 : KENS Experiment 2: Evaluation of spectra of high energy neutrons using the radioactive spallation products on Au**

Matsumura, H.<sup>a</sup>, Masumoto, K.<sup>a</sup>, Nakao, N.<sup>a</sup>, Toyoda, A.<sup>a</sup>, Kawai, M.<sup>a</sup>, Aze, T.<sup>b</sup>, Fujimura, M.<sup>c</sup> (<sup>a</sup>KEK, <sup>b</sup>The Univ. of Tokyo, <sup>c</sup>Nihon Univ.)

We carried out a shielding experiment of high-energy neutrons, which were generated from a tungsten target bombarded with primary 500-MeV protons at KENS, and penetrated through the concrete shield in the zero-degree direction. We propose a new method to evaluate the spectra of high-energy neutrons ranging from 8 to 500 MeV. Au foils were set in a concrete shield, and the reaction rates for 13 radionuclides produced by the spallation reactions on the Au targets were measured by radiochemical techniques. The experimental results were compared with those obtained by the MARS14 Monte-Carlo code. A good agreement between them was found in the neutron spectra above 100 MeV. The profile of the neutron spectrum, ranging from 8 to 500 MeV, does not depend on the thickness of the concrete shield during the penetration.

#### **1A08 : KENS Experiment 3: Development of Cl-36 AMS system and Evaluation of Cl-36 production rates in KENS concrete shieldings**

Aze, T.<sup>a</sup>, Fujimura, M.<sup>b</sup>, Noguchi, M.<sup>b</sup>, Matsumura, H.<sup>c</sup>, Nagai, H.<sup>d</sup>, Matsuzaki, H.<sup>e</sup>, Masumoto, K.<sup>c</sup>, Nakao, N.<sup>c</sup>, Kawai, M.<sup>c</sup> (<sup>a</sup>Graduate school of sci., Univ. of Tokyo, <sup>b</sup>Graduate School of Integrated Basic Sci., Nihon Univ., <sup>c</sup>KEK, <sup>d</sup>Coll. of Humanities and sci., Nihon Univ., <sup>e</sup>Res. Center for Nucl. Sci. and technol., The Univ. of Tokyo)

We developed a high sensitive and high effective  $^{36}\text{Cl}$  AMS(Accelerator Mass Spectrometry) system at MALT, The University of Tokyo. This system was applied to the shielding experiment of high-energy neutrons at KENS, High Energy Accelerator Research Organization.  $\text{CaCO}_3$  and  $\text{NaCl}$  targets were set at various depths of a concrete shield, and were irradiated with neutrons generated from a tungsten target bombarded with primary 500 MeV protons. After the irradiation, the concentrations of  $^{36}\text{Cl}$  produced in the targets were measured by the AMS system, and depth profiles for both targets were obtained. As a result, the reaction rate of Cl target was two orders higher than Ca target, however, both depth profiles were similar.

#### **1A09 : Study on isotope ratio measurement of ultra trace amounts of nuclear materials by ICP-MS**

Magara, M, Ichimura, S, Hirayama, F, Kurosawa, S, Esaka, F, Sakurai, S, Watanabe, K, Usuda, S. (JAERI)

JAERI has been developing analytical techniques for ultra-trace amounts of nuclear materials in environmental samples in order to contribute to the strengthened safeguards system of the IAEA. The isotope ratios of the nuclear materials in the environmental samples are measured because they give useful information about undeclared nuclear activities. Inductively coupled plasma mass spectrometer (ICP-MS) is a powerful tool for this purpose, however, co-existing elements and polyatomic ions resulting from impurities such as Pb frequently interfere with the isotope ratio measurement. The authors have measured the production ratio of polyatomic ions and investigated how to reduce the interference on the ICP-MS measurement in order to obtain the accurate isotope ratios. The production ratio of  $\text{PbO}_2^+$  to  $\text{Pb}^+$  was  $3 \times 10^{-8}$ , which interfered with the measurement of  $^{236}\text{U}$ ,  $^{238}\text{U}$ ,  $^{239}\text{Pu}$ ,  $^{240}\text{Pu}$  when the concentration of Pb in the sample to be measured with ICP-MS was more than 1  $\mu\text{g}/\text{ml}$ . The methods to reduce the interferences will be discussed.

#### **1A10 : Application of FT-TIMS method to environmental sample analysis for safeguards -2-**

Lee,C.G, Iguchi,K., Esaka,K.T, Inagawa,J., Suzuki,D., Esaka,F., Magara,M., Sakurai,S., Watanabe,K., Usuda,S. (JAERI)

Japan Atomic Energy Research Institute (JAERI) was authorized as a member of the network analytical laboratories (NWALs) of IAEA in January 2000 for analysis of safeguards environmental samples. Particle analysis is an effective method for safeguards because the isotope ratios of nuclear materials in individual particles can be determined. Secondary ion mass spectrometry (SIMS) is known as an analytical technique for particle analysis, however, it is difficult to analyze the particles with sub-micrometer diameter because of the detection limit.

As for the detection and the isotope ratio measurement of sub-micrometer particles, we are developing an analytical method using a combination of fission track (FT) technique and thermal ionization mass spectrometry (TIMS). In FT-TIMS method, the detection of fissile materials is affected by the etching condition of detector. In this study, as a first step, the influence of uranium enrichment to etching condition of fission track detector made of polycarbonate was investigated. The results obtained suggested that the screening of the uranium particles according to the enrichment is possible by controlling the etching time.

#### **1A11 : Photon activation analysis of carbon in atmospheric suspended particulate matters**

Oura, Y., Nagahata, T., Ebihara M. (Tokyo Metropolitan Univ.)

Total carbon contents in atmospheric suspended particulate matters ( $PM_{10}$ ) was determined by instrumental photon activation analysis.  $PM_{10}$  particles were collected on a quartz filter at Hachioji, Tokyo, for 5 days every other week since September, 2002. The particles on the filter were irradiated by bremsstrahlung with 20 MeV of end point energy for 20 min., then gamma spectrometry was performed immediately. Feature of a variation of carbon concentrations in atmosphere (in  $\mu g/m^3$ ) was almost similar with that of concentrations in particulates (in  $\mu g/g$ ). Though particulate concentrations were approximately constant between 20 and 35  $\mu g/m^3$ , carbon concentrations were fluctuated drastically (min.: 3.7  $\mu g/m^3$  and max.: 11  $\mu g/m^3$ ). Such fluctuation of carbon concentrations was suggested that particulates were resulted from a multiple origin. In addition to nondestructive analysis, it was tried to determine polycyclic aromatic hydrocarbons using extraction by dichloromethane after irradiation. 0.5% of total carbon was found to be extracted by dichloromethane.

#### **1A12 : Development of $\gamma$ -ray spectrum analysis program for neutron activation analysis**

Suzuki, S., Okada, Y., Hirai, S. (Faculty of Engineering, Musashi Institute of Technology)

The  $\gamma$ -ray spectrum analysis program by the personal computer for neutron activation analysis has been developed. The  $\gamma$ -ray peaks of the spectrum are searched automatically by inputting analytical conditions. The area of  $\gamma$ -ray peaks is analyzed by means of a fitting technique based on a non-linear least squares method. As a result, peaks, energies, and their intensities are calculated. Their intensities can be corrected for decay of the corresponding nuclide. Contents and concentrations of elements of interest in the sample are calculated by comparison with the intensities of standard samples. The overlapping multiple peaks have been analyzed precisely and easily by this program.

#### **1A13 : Neutron induced prompt gamma ray analysis of B in atmospheric suspended particulate matters**

Iguchi, H.<sup>a</sup>, Nagahata, T.<sup>a</sup>, Oura, Y.<sup>a</sup>, Otoshi, T.<sup>b</sup>, Ebihara, M.<sup>a</sup> (\*Tokyo Metropolitan Univ., <sup>b</sup>Tohoku Univ. of Comm.Serv. Sci.)

Boron in atmospheric suspended particulate matters ( $PM_{10}$ ) were determined by neutron induced prompt gamma ray activation analysis (PGA). Particulate matters were collected at Hachioji, Tokyo, and Sakata, Yamagata prefecture, for several days every other week by using 2 polycarbonate filters with different pore size (8 and 0.4  $\mu m$ ). A half of the filter on which particulates were collected were put into a FEP bug, then irradiated by thermal or cold neutrons for 3 to 6 hours at PGA system, JRR-3M. Boron concentration was found to be about 5  $ng/m^3$  both at Hachioji and at Sakata. In spring and summer, concentrations were tend to increase. This tendency was prominence at Sakata and concentrations at Sakata on August in 2003 was reached into about 20  $ng/m^3$ . Since boron was distributed in fine particles than coarse particles, most particulates including boron was presumable to be originated from artificial origin.

#### **1B01 : Correlation between thermal annealing behavior of radiation defects and tritium release behavior in neutrton-irradiated LiAlO<sub>2</sub>**

Nishikawa, Y.<sup>a</sup>, Oyadzu, M.<sup>a</sup>, Kimura, H.<sup>a</sup>, Munakata, K.<sup>b</sup>, Nishikawa, M.<sup>b</sup>, Okada, M.<sup>c</sup>, Moriyama, H.<sup>d</sup>, Okuno, K.<sup>a</sup> (\*Radiochemical Res. Lab., Fac. of Sci., Shizuoka Univ., <sup>b</sup>Dept.of Adv. Energy Eng. Sci., Kyushu Univ., <sup>c</sup>Res. Reactor Inst., Kyoto Univ., <sup>d</sup>Grad. Sch. Eng., Kyoto Univ)

In the blanket systems for D-T fusion reactors, hot tritium is produced mainly in Li-bearing materials by the reaction of  $^6Li(n,\alpha)^7T$ . For establishing the tritium recovery system, it is a critical issue to elucidate the chemical behavior of tritium produced in the materials, such as its existing states and migration. In our previous studies, we revealed that annihilation processes of radiation defects induced by neutron irradiation played an important role in the tritium release processes of lithium containing ceramics, such as  $Li_2O$ ,  $Li_4SiO_4$ ,  $Li_2ZrO_3$ . In the present study, the sample,  $LiAlO_2$ , is one of candidates for solid tritium breeding materials. The annihilation processes were studied by means of ESR (Electron Spin Resonance). The annealing experimental results indicated that the radiation defects produced in  $LiAlO_2$  were annihilated thermally in the two processes with fast and slow annihilation rates. In the presentation, we will discuss details of kinetics of the slow annihilation process, which is expected to correlate closely with the tritium release process.

### **1B02 : Dynamic behavior of energetic hydrogen isotope in Si<sub>3</sub>N<sub>4</sub>**

Masuhara,A.<sup>a</sup>,Kimura,H.<sup>b</sup>,Onishi,Y.<sup>b</sup>,Oya,Y.<sup>c</sup>,Okuno,K.<sup>b</sup>,Tanaka,S.<sup>d</sup>

(<sup>a</sup>Fac.of Sci., Tokyo Univ. of Sci., <sup>b</sup>Radiochem. Res. Lab., Shizuoka Univ., <sup>c</sup>Radioisotope Center, The Univ.of Tokyo, <sup>d</sup>Grad. School of Eng, The Univ.of Tokyo)

Silicon nitride (Si<sub>3</sub>N<sub>4</sub>) have good chemical stability and mechanical property in high temperature environment and is applied for various fields. However, the detailed mechanism, especially interaction mechanism with impurities, especially hydrogen, has not been elucidated. In this research, dynamic behavior and chemical existing states of energetic deuterium into Si<sub>3</sub>N<sub>4</sub> were studied by X-ray photoelectron spectroscopy (XPS) and thermal desorption spectroscopy (TDS). The 1.0 keV deuterium ions (D<sub>2</sub><sup>+</sup>) were implanted into β-Si<sub>3</sub>N<sub>4</sub> at an ion flux of  $1.27 \times 10^{18}$  D<sup>+</sup>/m<sup>2</sup>s up to an ion fluence between  $0.13 \times 10^{22}$  D<sup>+</sup>/m<sup>2</sup> and  $1.00 \times 10^{22}$  D<sup>+</sup>/m<sup>2</sup>. After D<sub>2</sub><sup>+</sup> implantation, the chemical states of N 1s and Si 2p were studied by XPS. The deuterium desorption behavior was also analyzed by TDS. Three desorption peaks were observed at around 400 K, 800 K and 1000 K. In the XPS analysis, the N 1s and Si 2p peaks were shifted to lower energy side by interacting with deuterium. These facts indicate that deuterium ions were bound to Si and N with forming Si-D and N-D bonds, respectively. The detailed mechanism will be discussed.

### **1B03 : Studies on hot atom chemical behavior of energetic ions in solids(VI)-Impurity effects for chemical behavior of energetic deuterium implanted in boron coating film-**

Miyauchi, H.<sup>a</sup> Yoshikawa, A.<sup>a</sup> Oyaidzu, M.<sup>a</sup>, Kimura, H.<sup>a</sup>Takeda, T.<sup>a</sup> Oya, Y.<sup>b</sup>, Sagara, A.<sup>c</sup>, Noda, N.<sup>c</sup>, and Okuno, K.<sup>a</sup>, (<sup>a</sup>Radiochemistry Research Laboratory, Faculty of Science, Shizuoka University, <sup>b</sup>Radioisotope Center, The University of Tokyo, <sup>c</sup>National Institute for Fusion Science)

For D-T fusion devices, boronization is to be considered to carry out to remove impurities, especially oxygen from plasma. Therefore, oxygen trapped in the boron coating film would be supposed to make a strong influence on the tritium retention and the trapping mechanism. In this study, pure and oxygen contaminated boron coating films (with and without oxygen ratio < ~2%, >~10%) were achieved by the plasma CVD device, and deuterium ion was implanted into these films. The chemical states of boron were evaluated by XPS and the deuterium desorption behavior was also studied by TDS. For the XPS results, the B1s peak top energy for both samples were shifted to the high-energy side by the deuterium implantation compared to that for the pure boron coating film. For the TDS results, two desorption stages of implanted deuterium were confirmed and ratio of desorbed amounts from these

stages depended on the concentration of oxygen impurity.

### **1B04 : Radiochemical study on low temperature reactions of H and T atoms formed by <sup>3</sup>He(n,p)<sup>3</sup>H in liquid helium at 1.6K**

Aratono, Y.<sup>a</sup> Iguchi, K.<sup>a</sup> Okuno, K.<sup>b</sup> (<sup>a</sup>JAERI, <sup>b</sup>Radiochem. Res. Lab., Shizuoka Univ.)

Helium shows very unique properties at condensed states (low temperature, superfluidity, low poralizability, large zero point motion, bubble atom, snowball, etc). Physicochemical behaviors of atoms, molecules and ionic species in liquid and solid helium are one of the current topics in low temperature chemistry in quantum medium. Radiochemical methods were applied to low temperature chemical reactions of H and T atoms formed by <sup>3</sup>He(n, p)<sup>3</sup>H(T) in liquid <sup>3</sup>He-<sup>4</sup>He mixture solution at 1.6K. An influence of superfluidity was observed in the recombination reaction of H + T → HT and T + T → T<sub>2</sub>. On the basis of preferential formation of HT over T<sub>2</sub> and a computer simulation of relative rate constants, formation of hydrogen isotope bubbles and their tunneling recombination were proposed. Two nuclear spin isomers of T<sub>2</sub> molecule, ortho-T<sub>2</sub> and para-T<sub>2</sub>, were found and the yield of the former was more than 90% , exceeding the statistical ratio at room temperature (75%). This non-statistical formation of ortho-T<sub>2</sub> molecule might be ascribed to the selective formation of odd-number rotational states in the excited complex.

### **1B05 : Abnormal Electronic X-ray Emission from Pionic Atom**

Ninomiya, K.<sup>a</sup> Sugiura, H.<sup>a</sup> Kasamatsu, Y.<sup>a</sup> Kikunaga, H.<sup>b</sup> Kinoshita, N.<sup>b</sup> Tani, Y.<sup>a</sup> Hasegawa, H.<sup>a</sup> Yatsukawa, M.<sup>a</sup> Takamiya, K.<sup>c</sup> Sato, W.<sup>a</sup> Matsumura, H.<sup>d</sup> Yoshimura, T.<sup>a</sup> Yokoyama, A.<sup>e</sup> Sueki, K.<sup>f</sup> Hamajima, Y.<sup>g</sup> Miura, T.<sup>d</sup> Shinohara, A.<sup>a</sup> ( <sup>a</sup>Grad. School Sci., Osaka Univ., <sup>b</sup>Grad. School Natural Sci., Kanazawa Univ., <sup>c</sup>Res. Reactor Inst., Kyoto Univ., <sup>d</sup>Res. Center Radiation, KEK, <sup>e</sup>Faculty Sci., Kanazawa Univ., <sup>f</sup>Dept. Chem., Univ. Tsukuba, <sup>g</sup>LLRL, Inst. Nature and Env. Technol., Kanazawa Univ.)

Our group has been studying a negative pion capture process in molecules. By measuring the electronic X rays, we attempt to reveal the electron rearrangement process in pionic atoms during the pion cascade. In the latest study, unexpected peaks are detected in some targets. These energies are quite similar to electronic X-ray energies of Z-2 atoms : Z is the atomic number of target atom. These X rays were measured only in a few targets, i.e. they were detected in Ho, Yb and Ta targets and not detected in Dy, Hg and other targets.

### **1B06 : Application of the on-line perturbed angular**

## **correlation method to condensed matter studies**

Sato, W.<sup>a,b</sup> Ueno, H.<sup>a</sup> Watanabe, H.<sup>a</sup> Miyoshi, H.<sup>c</sup> Yoshimi, A.<sup>a</sup> Kameda, D.<sup>c</sup> Kaihara, J.<sup>c</sup> Shimada, K.<sup>c</sup> Ito, T.<sup>c</sup> Suda, S.<sup>c</sup> Kobayashi, Y.<sup>a</sup> Shinohara, A.<sup>b</sup> Asahi, K.<sup>a,c</sup> (<sup>a</sup>RIKEN, <sup>b</sup>Grad. School Sci., Osaka Univ., <sup>c</sup>Dept. Phys., Tokyo Inst. Tech.)

The on-line time-differential perturbed-angular-correlation (TDPAC) method using a newly developed probe of <sup>19</sup>F was applied to the study of condensed matter physics by means of the ion-implantation method by combined use of the Ring Cyclotron and the RIKEN projectile-fragment separator. Powder fullerene C<sub>60</sub> and a sheet of highly oriented pyrolytic graphite (HOPG) were first adopted as the test samples for the experiment. The TDPAC spectra have shown contrastive behavior of the probe nucleus implanted in those carbon allotropes. For powder C<sub>60</sub>, the nucleus feels temperature-independent dynamic perturbation, while one has a static interaction with the surrounding extranuclear field for HOPG. Showing detailed experimental results for other samples as well as the carbon allotropes, we discuss the applicability of this on-line method to wider condensed matter studies.

## **1B07 : Application of coincidence Doppler broadening spectroscopy to positron annihilation**

Suzuki, T., <sup>a</sup>Yu, R.S., <sup>a</sup>Djourelov, N., <sup>a</sup>Kondo, K., <sup>a</sup>Ito, Y.<sup>a</sup> (<sup>a</sup>KEK)

The CDBS technique was applied to study the electron momentum distribution in simple hydrocarbons: cyclohexane, normal hexane, cyclohexanone and benzene. Considerable change in the Ps annihilation component of the DB curve was found as due to annihilation on electrons of carbonyl groups of cyclohexanone. Considering the CDBS ratio of positron annihilation in solid and liquid, electron momentum distribution of pick-off annihilation in a bubble can be deduced. The presence of  $\pi$  in addition to  $\sigma$  valence electrons broadened the electron momentum distribution. The last was also detected as a change in the shape of the CDBS ratio

## **1B08 : Preparation and half-life measurement of samarium-146**

Kinoshita, N.<sup>a</sup> Amakawa, H.<sup>b</sup> Hashimoto, T.<sup>a</sup> Takahashi, N.<sup>c</sup> Yokoyama, A.<sup>a</sup> and Nakanishi, T.<sup>a</sup> (<sup>a</sup>Grad. School Natural Sci. Tech., Kanazawa Univ., <sup>b</sup>Dept. Chem., Grad. School Sci., Tokyo Metro. Univ., <sup>c</sup>Grad. School Sci., Osaka Univ.)

Samarium-146 is known as an extinct nuclide in the present solar system. The half-life value currently adopted for this nuclide was determined in 1966 to be  $(1.03 \pm 0.05) \times 10^8$  y, but the half-life of Sm-146 has not been reevaluated since 1967. In order to renew the data,

Sm-146 was produced from two methods different from previous works and reevaluation of the half-life was attempted. Sm-146 was prepared from naturally occurring Sm-147 nuclide, a long-lived alpha emitter, in the  $^{147}\text{Sm}(\gamma, n)^{146}\text{Sm}$  reaction and the  $^{147}\text{Sm}(p, 2n)^{146}\text{Eu} \rightarrow ^{146}\text{Sm}$  reaction. After the preparation of Sm-146, the Sm-146 sample was precipitated in ammonia water and collected on a membrane filter for preparation of counting source. Alpha spectrometry using a Si semiconductor detector was carried out to determine alpha activity ratio of <sup>146</sup>Sm/<sup>147</sup>Sm. A portion of the Sm-146 sample was subjected to mass spectrometry using TIMS for <sup>146</sup>Sm/<sup>147</sup>Sm atomic ratio. In the mass spectrometry, Nd-146 was found to interfere in determination of Sm-146. The upper limit of the half-life was thus far obtained to be  $1.4 \times 10^9$  y.

## **1B09 : Adsorption behavior of trivalent lanthanides and actinides on tertiary pyridine resin and effect of alcohol addition**

Suzuki, T., <sup>a</sup>Ikeda, A., <sup>a</sup>Itoh, K., <sup>a</sup>Otake, K., <sup>a</sup>Aida, M., <sup>a</sup>Fujii, Y., <sup>a</sup>Hara, M., <sup>b</sup>Mitsugashira, T., <sup>b</sup>Ozawa, M.<sup>a,c</sup> (Tokyo Tech.<sup>a</sup>, Tohoku Univ.<sup>b</sup>, JNC<sup>c</sup>)

The adsorption behaviors of rare earth elements and trivalent actinides on the tertiary pyridine type resin with the hydrochloric acid / methanol mixed solution and the nitric acid / methanol mixed solution were investigated. The adsorption behavior of these elements in the nitric acid system is governed by their ionic radii, while, in the hydrochloric acid system, the distribution coefficients of 4f-elements and 5f-elements are completely different, i.e., 5f-elements have much larger distribution coefficients. The alcohol addition effect on adsorption in both systems was also investigated. In both systems, the distribution coefficients increase with alcohol concentration. The hydration numbers of erbium ion in alcoholic solution were diagnosed by EXAFS. As a result, the hydration numbers on inner sphere were scarcely varied with alcohol concentration. This result shows that the adsorption behaviors of these ions cannot be explained only by coordination of inner sphere.

## **1B10 : Interactions of europium(III) and curium(III) with the cell surfaces of microorganisms examined by time-resolved laser-induced fluorescence spectroscopy (TRLFS)**

Ozaki, T., <sup>a</sup>Kimura, T., <sup>b</sup>Ohnuki, T., <sup>a</sup>Francis, A.J.<sup>c</sup> (<sup>a</sup>Adv. Sci. Res. Center, JAERI, <sup>b</sup>Dep. Mater. Sci., JAERI, <sup>c</sup>Environ. Sci. Dep., BNL)

We investigated the association of europium(III) and curium(III) with *Chlorella vulgaris*, *Bacillus subtilis*, *Pseudomonas fluorescens*, *Halomonas* sp., *Halobacterium salinarum*, and *Halobacterium halobium*. We determined the kinetics and distribution coefficients (K<sub>d</sub>)

for Eu(III) and Cm(III) sorption at pH 3-5 by batch experiments, and evaluated the number of H<sub>2</sub>O in the inner-sphere (N<sub>H<sub>2</sub>O</sub>) and the degree of strength of ligand field (R<sub>EM</sub>) for Eu(III) by TRLFS. Exudates from *C. vulgaris* had an affinity for Eu(III) and Cm(III). The halophilic microorganisms showed almost no pH dependence in log K<sub>d</sub>, indicating that an exchange with Na<sup>+</sup> on the functional groups was involved in their sorption. The N<sub>H<sub>2</sub>O</sub> for Eu(III) on *C. vulgaris* was 6-8, while that for the other microorganisms was 3-6. The R<sub>EM</sub> for Eu(III) on halophilic microorganisms was 2.5-5, while that for non-halophilic ones was 1-2.5. This finding suggests that the coordination environment of Eu(III) on the halophilic microorganisms is more complicated than that on the other three non-halophilic ones.

### **1B11 : Study on separation of trivalent 4f and 5f block element ions by a paper electrophoresis**

Ishii, Y.<sup>a</sup> Miyashita, S.<sup>a</sup> Matsuyama, K.,<sup>a</sup> Mori, T.<sup>a</sup> Yanaga, M.,<sup>b</sup> Satoh, I.,<sup>c</sup> Suganuma, H.<sup>b</sup> (<sup>a</sup>Grad. Sch. of Sci. and Eng., Shizuoka Univ., <sup>b</sup>Fac. of Sci., Shizuoka Univ., <sup>c</sup>IMR, Tohoku Univ.)

The migration velocity of Eu<sup>3+</sup> and Am<sup>3+</sup> was measured in a mixed (methanol + H<sub>2</sub>O) solution containing 0.1 M HClO<sub>4</sub> + 0 ~ 1.0 M NaClO<sub>4</sub> or 0.1 M HClO<sub>4</sub> + 0 ~ 1.0 M NaI by a paper electrophoresis. The migration velocity of both ions decreased with increasing the fraction of methanol in 0 ~ 40 vol. % of methanol in the mixed solution. A difference between the migration velocities of Eu<sup>3+</sup> and Am<sup>3+</sup> was observed in NaI solution. It is thought that I<sup>-</sup> interacts electrostatically with the migration ions more effectively than ClO<sub>4</sub><sup>-</sup> because I<sup>-</sup> has a smaller crystallographic radius relative to ClO<sub>4</sub><sup>-</sup>. And as Am<sup>3+</sup> has somewhat covalency compared with Eu<sup>3+</sup>, it can be presumed that the outside of the first solvation shell of Am<sup>3+</sup> has a larger positive charge than that of Eu<sup>3+</sup>. So, it may be concluded that the stronger interaction between Am<sup>3+</sup> and I<sup>-</sup> results in a lowering of the migration velocity for Am<sup>3+</sup>.

### **1B12 : Development of a pH-Eh stat system to study actinide chemistry in aqueous solution**

Kirishima, A., Kitatsuji, Y. and Kimura, T. (JAERI)

Redox potential Eh is one of the most important thermodynamic factors as well as pH and ionic strength. Since uranium, neptunium and plutonium take various oxidation states in aqueous solution, Eh shift of solution system changes their chemical behaviors drastically. To study actinide's reactions going with Eh shift in pH region more quantitatively, the present work focuses on the development of a pH-Eh stat system which makes it possible to set Eh and pH values arbitrarily and keep them constantly. The system consists of two automatic burettes injecting acid or alkaline solution, supporting redox pair such as [Fe<sup>3+</sup>/Fe<sup>2+</sup>] or

[Fe(EDTA)<sup>-</sup>/Fe(EDTA)<sup>2-</sup>] and bulk potentiostatic electrolysis equipment made up of a potentiostat and a Pt-black working electrode etc. Impressed voltage on the working electrode controls the fraction of supporting redox pair, which determines Eh of the system. The redox pair [Fe<sup>2+</sup>/Fe<sup>3+</sup>] has enabled to stat Eh in a range from 600 mV (vs. SHE) to 950 mV at pH 1.77 ± 0.02. Since complexation of EDTA makes the standard redox potential E' of [Fe(EDTA)<sup>-</sup>/Fe(EDTA)<sup>2-</sup>] shift negatively, the adjustable Eh range by this redox pair has been 84 ≤ Eh /mV ≤ 580 at pH 4.00 ± 0.04.

### **1B13 : The resonance Raman effect of uranyl compounds**

Soga, T. (Japan Atomic Energy Research Institute)

The resonance Raman scattering spectra of uranyl compounds in dimethyl sulfoxide have been measured under laser excitation of the UO<sub>2</sub><sup>2+</sup> ion in resonance with the  $^1\Sigma_g^+ \rightarrow ^1\Phi_g$  Laport-forbidden f-f electronic transitions span from 510 to 450 nm. The resonance Raman excitation profile of the totally symmetric stretching vibrational mode of uranyl is presented and analyzed in terms of transform theory within the non-Condon model to give relatively good agreement with experimental results. Reliable value of the amount of charge transferred from the ligand to uranium of uranyl ion both in the ground and excited states are obtained. It is found that, in the  $^1\Sigma_g^+ \rightarrow ^1\Phi_g$  electronic transition, the amount of charge transferred from ligands to uranyl is related to the magnitude of the change in the excitation profile.

### **1P01 : Development of online solvent extraction system for heavy actinide chemistry**

Saiki, D.<sup>1</sup>, Kitamoto, Y.<sup>1</sup>, Matsuo, K.<sup>1</sup>, Tani, Y.<sup>1</sup>, Hasegawa, H.<sup>1</sup>, Sato, W.<sup>1</sup>, Takahashi, N.<sup>1</sup>, Yoshimura, T.<sup>1</sup>, Takimiya, K.<sup>2</sup>, Shibata, S.<sup>2</sup>, Haba, H.<sup>3</sup>, Enomoto, S.<sup>3</sup>, Shinohara, A.<sup>1</sup> (Grad. School of Science, Osaka Univ.<sup>1</sup>, Res. Reactor Inst., Kyoto Univ.<sup>2</sup>, RIKEN<sup>3</sup>)

We have developed an online rapid chemical operation system for heavy actinide elements. On this study, the online experiment was made in RIKEN Ring Cyclotron using solvent extraction of TTA complexes of lanthanide elements to toluene phase. Then the result was consistent with that of the batch experiments.

### **1P02 : Development of electrochemical method by a flow-electrolytic-column for heavy elements**

Matsuo,K<sup>a</sup>., Toyoshima,A<sup>a,b</sup>., Sato,W<sup>a</sup>., Takahashi,N<sup>a</sup>., Yoshimura,T<sup>a</sup>., Shinohara,A<sup>a</sup>., Tsukada,K<sup>b</sup>., Asai,M<sup>b</sup>., Akiyama,K<sup>b</sup>., Nishinaka,I<sup>b</sup>., Nagame,Y<sup>b</sup>.(Osaka Univ.<sup>a</sup>, Advanced Sci. Res. Center, JAERI<sup>b</sup>)

We are developing a new electrochemical method with a flow-electrolytic-column for heavy elements. As a simulation about the

oxidation of heavy actinide element No(nobelium), the oxidation of career-free Ce tracer was made with a flow-electrolytic-column and Ce<sup>4+</sup> was separated from Ce<sup>3+</sup> by cation exchange. As a result, we could confirm that the fraction of Ce<sup>4+</sup> increased in proportion to the applied voltage. We will also represent the result of on-line No experiment.

### 1P03 : Search for rapid preparation method of $\alpha$ source

Saito, J., Goto, S., Kudo, H. (Fac. of Sci., Niigata Univ.)

In order to prepare thin and uniform  $\alpha$  source rapidly after chemical separation of transactinide elements, we fabricated an apparatus spraying and drying a liquid sample in vacuum. If sample solution is sprayed on to a filter paper, a collection efficiency is about 100%. But the collection efficiency at high temperature is about 30%. We searched optimum conditions such as flow rate of spraying and drying temperature, so that the collection efficiency is increased to about 80%. But we have still a problem with reproducibility, and we will discuss about it.

### 1P04 : Heavy element search using the $^{208}\text{Pb} + ^{70}\text{Zn}$ reaction

Kaji, D.,<sup>a</sup> Morita, K.,<sup>a</sup> Morimoto, K.,<sup>a</sup> Akiyama, T.,<sup>b</sup> Goto, S.,<sup>c</sup> Haba, H.,<sup>a</sup> Ideguchi, E.,<sup>d</sup> Koura, H.,<sup>c</sup> Kudo, H.,<sup>c</sup> Ohnishi, T.,<sup>a</sup> Ozawa, A.,<sup>f</sup> Suda, T.,<sup>a</sup> Sueki, K.,<sup>f</sup> Xu, H.,<sup>g</sup> Yamaguchi, T.,<sup>b</sup> Yoneda, A.,<sup>a</sup> Yoshida, A.,<sup>a</sup> Zhao, Y.-L.,<sup>h</sup> (RIKEN, <sup>b</sup>Saitama Univ., <sup>c</sup>Niigata Univ., <sup>d</sup>Univ. of Tokyo, <sup>e</sup>JAERI, <sup>f</sup>Univ. of Tsukuba, <sup>g</sup>IMP, <sup>h</sup>IHEP)

A gas-filled recoil separator (GARIS) for heavy element research was installed at an experimental hall of the RIKEN linear accelerator (RILAC) facility. One of the interesting applications of the separator is the discovery of nuclei of super-heavy elements whose atomic number are greater than 112. We performed an experiment to study production and decay of  $^{277}\text{112}$  produced by the  $^{208}\text{Pb}(^{70}\text{Zn}, \text{n})^{277}\text{112}$  reaction.

### 1P05 : Development of liquid scintillation counting system for the on-line $\alpha$ -ray measurement of heavy elements

Tani, Y., Hasegawa, H., Saika, D., Kitamoto, Y., Matsuo, K., Sato, W., TakahashiA, N., Yoshimura, T., Haba, H., Shinohara, A. (Grad. School of science, Osaka Univ., RIKEN)

Liquid extraction system and high-sensitive flow liquid scintillation counting system were developed for the purpose to perform the on-line chemical experiment of heavy elements rapidly, automatically, and repeatedly.  $\beta$ -ray discrimination on liquid scintillation counting enabled to detect  $\alpha$  rays at low background. We will also report the results of  $\alpha$ -ray measurements of  $^{150}\text{Dy}$  and  $^{151}\text{Dy}$  obtained from on-line chemical experiment at RIKEN Ring Cyclotron.

### 1P06 : Visible and ultraviolet light measurement from the ultra low-lying isomer $^{229m}\text{Th}$

Kasamatsu, Y.,<sup>1</sup> Kikunaga, H.,<sup>2</sup> Takamiya, K.,<sup>3</sup> Mitsugashira, T.,<sup>4</sup> Nakanishi, T.,<sup>2</sup> Ohtsuki, T.,<sup>5</sup> Yuki, H.,<sup>5</sup> Haba, H.,<sup>6</sup> Sato, W.,<sup>1</sup> Yamana, H.,<sup>3</sup> Ohkubo, Y.,<sup>3</sup> Hara, M.,<sup>4</sup> Ninomiya, K.,<sup>1</sup> Shibata, S.,<sup>3</sup> Shinohara, A.<sup>1</sup> (<sup>1</sup>Grad. School Sci., Osaka Univ., <sup>2</sup>Grad. School Nat. Sci. Tech., Kanazawa Univ., <sup>3</sup>Res. Reactor Inst., Kyoto Univ., <sup>4</sup>The Oarai-branch, Inst. Materials Res., Tohoku Univ., <sup>5</sup>Lab. Nucl. Sci., Grad. School Sci., Tohoku Univ., <sup>6</sup>RIKEN)

A Low-lying isomer  $^{229m}\text{Th}$  is expected to have a unique property that the decay process varies depending on its chemical state; it could be a good subject of the investigation of an electron bridge mechanism. We have tried to detect visible and ultraviolet photons emitted from  $^{229m}\text{Th}$  by a low-noise photomultiplier.  $^{229}\text{Th}$  sample was obtained as a decay product of  $^{233}\text{U}$  and by various nuclear reactions such as  $^{228}\text{Ra}(\text{n},\gamma)^{229}\text{Ra}$ ,  $^{232}\text{Th}(\gamma,\text{p}2\text{n})^{229}\text{Ac}$ .  $^{229}\text{Th}$  was purified by chemical separation for the photon detection. In the present work, we report the results of each photon measurement and quantitatively discuss on the half-life of  $^{229m}\text{Th}$  based on the detection limit.

### 1P07 : Search for the extremely low energy isomer of Th-229 by alpha-spectrometry

Kikunaga, H.,<sup>1</sup> Kasamatsu, Y.,<sup>2</sup> Takamiya, K.,<sup>3</sup> Mitsugashira, T.,<sup>4</sup> Hara, M.,<sup>4</sup> Ohtsuki, T.,<sup>5</sup> Yuki, H.,<sup>5</sup> Haba, H.,<sup>6</sup> Shinohara, A.<sup>2</sup> Shibata, S.,<sup>3</sup> Kinoshita, N.,<sup>1</sup> Yokoyama, A.,<sup>1</sup> Nakanishi, T.,<sup>1</sup> (<sup>1</sup>Grad. School Nat. Sci. Tech., Kanazawa Univ., <sup>2</sup>Grad. School Sci., Osaka Univ., <sup>3</sup>Res. Reactor Inst., Kyoto Univ., <sup>4</sup>The Oarai-branch, Inst. Materials Res., Tohoku Univ., <sup>5</sup>Lab. Nucl. Sci., Grad. School Sci., Tohoku Univ., <sup>6</sup>Cyclotron Center, RIKEN,)

We attempted to produce the extremely low energy isomer of Th-229 (Th-229m) in (1) Th-232(gamma, n) reaction, (2) Th-232(gamma, p2n)Ac-229, disintegrating to Th-229, reaction and (3)alpha-decay of U-233 for the purpose of determination of its half-life. The products above were isolated from irradiated targets by using several chemical separation methods and identified by alpha-spectrometry.

In the measured alpha-spectra, we observed some events in the region expected for Th-229m (4.85-5.05 MeV), and the decrease of alpha activity ascribed to Th-229m showed a half-life of about 10 hours (as a hydroxide form).

### 1P08 : EXAFS Study of the 4th and 5th Group of Elements in Hydrofluoric acid Solution

Akiyama, K.,<sup>a</sup> Haba, H.,<sup>b</sup> Tsukada, K.,<sup>a</sup> Asai, M.,<sup>a</sup> Sueki, K.,<sup>c</sup>

Toyoshima, A.,<sup>a,d</sup> Yaita, T.,<sup>a</sup> Nagame, Y.<sup>a</sup> (<sup>a</sup>Advanced Sci. Res. Center, JAERI, <sup>b</sup>Cyclotron Center, RIKEN, <sup>c</sup>Dep. of Chemistry, Univ. of Tsukuba, <sup>d</sup>Grad. School of Sci., Osaka Univ.)

We studied the molecular structure of the metal complexes for the group 4 elements of Zr and Hf, and the group 5 elements of Nb using Extended X-ray Absorption Fine Structure (EXAFS) method to discuss the anion exchange behavior of the element 104, Rf, and the element 105, Db, in the hydrofluoric acid. The metal sheets of Zr and Hf, and the fluoride salt of Nb were dissolved in the hydrofluoric acid solution and set for the EXAFS measurement on the BL27B beam line at Photon Factory (PF) of KEK in tsukuba. The radial structure functions of Zr and Hf evaluated from the observed EXAFS spectra are almost same as each other among 0.01 and 10 M of the hydrofluoric acid concentration. While those of Nb are gradually changed with the increase of the HF concentration.

#### 1P09 : Nuclear scission shapes of pair fragments in two fission modes

Nihsinaka, I.<sup>1</sup>, Nagame, Y.<sup>1</sup>, Nakahara, H.<sup>1</sup> (<sup>1</sup>Adv. Sci. Res. Cent., JAERI, <sup>2</sup>Tokyo. Metro. Univ.)

Primary and secondary fragment mass, fragment total kinetic energy, and neutron multiplicity have been measured in the 12 MeV proton induced fission of <sup>232</sup>Th. For symmetric and asymmetric fission modes partition of the total excitation energy between fragment pairs has been deduced from neutron multiplicity. Scission configurations composed of two touching spheroids have been evaluated from fragment excitation energies and total kinetic energy by calculating nuclear energy and Coulomb energy. Heavy fragments with A = 130 have quite different degrees of deformation corresponding to the two fission modes compared with the complementary light fragments with A = 103.

#### 1P10 : Basic studies on isothermal gas chromatography of group-4 elements

Ito, M., Goto, S., Kudo, H. (Fac. of Sci., Niigata Univ.)

The chemical properties of the group-4 elements, Rf, Zr and Hf in the gas-phase have been investigated using an isothermal gas chromatographic method, because their halides are volatile. In previous experiments, Cl<sub>2</sub>/CCl<sub>4</sub> was used as chlorinating reagent, but decomposed products of CCl<sub>4</sub> were crystallized inside the isothermal column and it was difficult to perform the experiment continuously. In the present work, Cl<sub>2</sub> or HCl gas was used as an alternative chlorinating reagent to Cl<sub>2</sub>/CCl<sub>4</sub>, and the possibility of application and the optimal reaction conditions were studied using Zr isotopes from <sup>252</sup>Cf

spontaneous fission. The volatile Zr compounds were observed by use of HCl and carbon wool as a reaction site. In this case any by-products were not observed. The reaction mechanism of formation of volatile compounds will be discussed.

#### 1P11 : Measurement of Etch Pit Profile in Solid State Nuclear Track Detector with an Atomic Force Microscope

Arai, M.,<sup>1</sup> Yokoyama, A.,<sup>1</sup> Kikunaga, H.,<sup>1</sup> Kinoshita, N.,<sup>1</sup> Hashimoto, T.,<sup>1</sup> Shinohara, A.,<sup>2</sup> Sato, W.,<sup>2</sup> Kasamatsu, Y.,<sup>2</sup> Yatsukawa, M.,<sup>2</sup> Shibata, S.,<sup>3</sup> Yasuda, N.<sup>3</sup> (<sup>1</sup>Graduate School of Natural Science and Technology, Kanazawa Univ., <sup>2</sup>Graduate School of Science, Osaka Univ., <sup>3</sup>National Institute of Radiological Sciences)

In measuring nuclear reaction products using a solid-state nuclear track detector, improvement of nuclide identification from information on etch-pit will make the method more useful in many research fields. In this study, using a SSNTD of CR-39 we investigated the relationship between nuclear reaction products and the information on the etch-pits observed with an atomic force microscope, which gives one information on the pits in size and depth. As an experiment, the plates of CR-39 were placed around a gold target, which was irradiated with <sup>12</sup>C beam of 290 MeV/u. Then, the plates of CR-39 were etched in NaOH solution. We found a group of tracks of a similar profile and the other tracks mainly in a position comparatively distant from the beam axis. The latter tracks vary in profile according to the distance from the beam axis.

#### 1P12 : Experimental evaluation of neutron self-absorption in gold target using UTR-KINKI

Murata, Y.,<sup>a</sup> Komura, K.,<sup>a</sup> Koga, T.,<sup>b</sup> Morishima, H.<sup>b</sup> (<sup>a</sup>LLRL, Kanazawa Univ., <sup>b</sup>Atomic Energy Res. Inst., Kinki Univ.)

In order to use gold as excellent neutron detector, self-absorption of neutrons in gold target was experimentally evaluated by using Kinki University nuclear reactor (UTR-KINKI). Seven gold grain samples, diameter of which were ranging from 0.8 to 3.4 mm, were irradiated 10 minutes by neutrons in center of UTR-KINKI (neutron flux:  $1 \times 10^7$  n·cm<sup>-2</sup>·s<sup>-1</sup>). Six gold plate samples, sizes of which were 40 × 150 × 0.1 mm, were irradiated by leakage neutrons for 6 hours at outer wall of UTR-KINKI (neutron flux:  $10$  n·cm<sup>-2</sup>·s<sup>-1</sup>). The <sup>198</sup>Au activities in the gold samples were measured by ultra low background γ-ray spectrometry at Ogoya Underground Laboratory. Relative <sup>198</sup>Au activities in gold grains decreased with the increase of diameter and/or thickness of gold target. Activities of a 3.4 mmφ grain sample was half of 0.8 mmφ sample, while decrease of <sup>198</sup>Au activities in gold plates were more slower than that in gold grains.

### **1P13 : Neutron activation analysis of Selenium in human toenails**

Ohno, S., Seki, R., (Department of Chemistry, University of Tsukuba)

Concentrations of Selenium (Se), an essential trace element in human nutrition, in human toenails of about 300 control individuals with ages ranging from 1 to 96 years living in Japan and China (Peking) and Taiwan were determined by instrumental neutron activation analysis. Statistical analysis demonstrated several different pattern of Selenium correlation with age and sex and living area. Concentration of Selenium was found to be negatively correlated with age, and to be higher in females than in males. The overall average toe nail specimens in Japan found in this study was found to be  $0.92 \pm 0.17$  ppm.

### **1P14 : Change of concentrations of trace elements in livers of zinc deficiency mice**

Minayoshi, R., Kinugawa, N., Ohyama, T., Ogi, T., Ishikawa, K., Noguchi, M., Saganuma, H., Takahashi, K., Enomoto, S., Yanaga, M. (Fac. of Sci., Shizuoka Univ. and RIKEN)

Concentrations of trace elements in livers of Zn deficient mice and control mice were investigated. Eight-week old male mice of ICR stain were divided into two groups. One group was fed with Zn-deficient diet, and the other group was fed with control diet. After three weeks, their livers were removed and weighed, immediately. Then, every eight livers of each group were together homogenized and divided into two subcellular fractions, such as supernatant and other fractions, by ultracentrifugation. The supernatant fraction was further divided into forty fractions by means of gel filtration chromatography. Then, the concentrations of the metallic elements and proteins in each fraction were determined by ICP-MS, and BCA protein assay method, respectively. Furthermore, SDS-PAGE was carried out for the fractions, No. 12~21. The concentrations of zinc in the 14, 15, 16, 21 and 22<sup>nd</sup> fractions of Zn-deficient mice were decreased, and the concentrations of cobalt were increased in the 14, 17, 18, 21, and 22<sup>nd</sup> fractions. BCA protein assay data showed that the concentrations of proteins in these fractions were decreased. However, no significant differences were found on gel after SDS-PAGE for the fractions, No. 12~21, of Zn-deficient and control mice.

### **1P15 : Change of concentrations of trace elements in pancreatic cell of zinc deficiency mice (II)**

Kinugawa, N., Minayoshi, R., Ogi, T., Kamishima, J., Ishikawa, K., Noguchi, M., Saganuma, H., Yanaga, M. (Fac. of Sci., Shizuoka Univ.)

Concentrations of various trace elements in pancreatic cells of Zn-deficient mice and control mice were determined. Eight-week old

male mice of ICR strain were divided into two groups, and fed with Zn-deficient diets and control diets, respectively. After three weeks keeping, their pancreata were removed and separated into 4 subcellular fractions, such as nucleus, mitochondria, microsome, and cytosol, by centrifugal method. Concentrations of 10 elements, Na, Mg, Cl, Mn Fe, Co, Zn, Se, Br and Rb, in each subcellular fraction, were determined by instrumental neutron activation analysis. Furthermore, SDS-PAGE was carried out for the cytosolic fractions. In all the subcellular fractions, The INAA results showed that zinc concentrations of Zn-deficient mice were lower than those of control mice and Co concentrations of Zn-deficient mice were higher than those of control mice. However, no significant differences were found for the positions and number of the cytosolic protein bands on the gel after SDS-PAGE. This suggests that the possibility of disappearance of specific proteins or induction of another proteins was low even under zinc deficient condition.

### **1P16 : Extractable organohalogens (EOX) and dioxins in waste ash samples: Comparison to chemical analyses (instrumental neutron activation analysis: INAA, and gas chromatography/mass spectrometry: GC/MS) and to a bioassay (ethoxyresorufin- O-deethylase: EROD assay)**

Kawano, M.<sup>a</sup>, Matsui, M.<sup>b</sup>, Kashima, Y.<sup>b</sup>, Matsuda, M.<sup>a</sup>, Ambe, K.<sup>c</sup>, Wakimoto, T.<sup>a</sup>, Doi, R<sup>b</sup> (<sup>a</sup>Department of Environment Conservation, Faculty of Agriculture, Ehime University, <sup>b</sup> Department of Hygiene, School of Medicine, Yokohama City University, <sup>c</sup>Department of Living Science, Nagano Prefectural College)

Various waste ash samples collected from medical, municipal and small-scale domestic incinerators were investigated for extractable organohalogens (EOX) and dioxins (polychlorinated dibenzo-p-dioxins: PCDDs; polychlorinated dibenzofurans: PCDFs; and coplanar polychlorinated biphenyls: Co-PCBs) and for dioxin-like activities using bioassay technique in order to evaluate potential toxicity and responsible chemicals in those samples. EOX analysis suggested that ash samples contained plenty of organohalogen compounds apart from PCDD/Fs and Co-PCBs. Some samples exhibited higher potency than expected from the chemical analysis (GC/MS). The results imply that some bioactive organohalogens that cannot be detected in the conventional chemical analysis might have potential for dioxin-like toxicities, and contribute to higher bioassay activities.

### **1P17 : Seasonal variation of the element concentration in the plant leaf by the Ko method**

Sugihara, S.<sup>a</sup>, Efrizal,<sup>a</sup> Osaki, S.<sup>b</sup>, Maeda, Y.<sup>a</sup> (<sup>a</sup>Faculty of Sciences, Kyushu Univ., <sup>b</sup>Radioisotope Center, Kyushu Univ.)

In order to search a new biomonitor, the various plants from which form is different were extracted, and the difference in the capture ability of the atmospheric aerosol and the seasonal variation of a content element were investigated. When a seasonal variation and the original change of a plant kind exist in a leaf content element, it is necessary to evaluate the variation of element concentration as a background. The natural radioactivity ( $^{7}\text{Be}$ ,  $^{210}\text{Pb}$ ,  $^{40}\text{K}$ ) in a leaf, total deposition and aerosol was measured simultaneously by the gamma ray spectrometry. Eight kinds of a plant leaf were collected near the Sefuri mountains top of Fukuoka Prefecture every month. The element concentrations were determined by a neutron activation analysis (Ko method). The two type of Irradiation ( 10 sec and 3 hour ) were performed. The seasonal variation of a content element was investigated and comparison examination was carried out about the relation with a radioactive nuclide.

#### **1P18 : The characteristics of Tc-Pn in KUR and their application to determination of trace manganese in high-purity iron**

Sekimoto, S.<sup>a</sup>, Kobayashi, T.<sup>b</sup>, Takamiya, K.<sup>c</sup>, Shibata, S.<sup>c</sup> (<sup>a</sup>Grad. School of Eng., Kyoto Univ., <sup>b</sup>College of Humanities and Sci., Nihon Univ., <sup>c</sup>Res. Reactor Inst., Kyoto Univ.)

Trace amount of manganese in high-purity iron was estimated by instrumental neutron activation analysis using Tc-Pn in Research Reactor Institute, Kyoto University. Accurate determination of that needs to subtract the interference by  $^{56}\text{Fe}(\text{n},\text{p})^{56}\text{Mn}$  reaction with fast neutron. Our group will now apply Tomura's method[1] to determine trace amount of manganese in the same sample accurately. Those method in Tc-Pn in KUR will be applicable to determination of trace amount of manganese in iron meteorites in the near future. Also the Cd(Au) ratio in Tc-Pn in KUR will be reported.

[1]Tomura, K. et al., Journal of Radioanal. and Nuclear Chem. Vol. 242, No. 1 (1999) 147-153.

#### **1P19 : Trace elements in Ruby and Sapphire samples from vietnam**

Hatsukawa Y<sup>a</sup>, Tran Van Luyen<sup>ab</sup>, Toh Y.<sup>a</sup>, Oshima M<sup>a</sup>. (<sup>a</sup>Japan Atomic Energy Research Institute, <sup>b</sup>Vietnam Atomic Energy Commission)

Ruby and Sapphire samples from Vietnam were collected at Lucyen mine (northern Vietnam) for Ruby, and Thuong Xuan area (southern Vietnam) for Sapphire. Recently, Japan Atomic Energy Research Institute (JAERI) has developed a high-sensitive non-destructive trace element analysis method based on multi-parameter gamma-ray coincidence detection. In this study we measured trace elements in Ruby and Sapphire samples using the multi-parameter coincidence

method. The Ruby and Sapphire samples were irradiated at JAERI's research reactor, JRR-3M. Gamma-rays from irradiated samples were measured at single Ge detector, and an Ge detectors array, GEMINI-II. We found forty five elements in the Ruby and Sapphire samples in this study. These trace elements in the samples vary between ruby and sapphire, and also among different color of sapphire samples. The patterns of lanthanide elements were obtained, and the patterns showed the differences between ruby and sapphire.

#### **1P20 : Time resolved prompt and decay gamma ray spectrometry using list mode measurement system**

Matsue, H (JAERI, Tokai)

We have studied discrete measurement of prompt and decay gamma rays using pulsed neutron beam generated by a neutron disk chopper in JRR-3M prompt gamma ray analysis system. In this study, list mode measurement system installed to the discrete measurement of prompt and decay gamma rays. Using this system, time resolved prompt and decay gamma ray spectrum can be acquired.

#### **1P21 : Development of accelerator mass spectrometry of $^{32}\text{Si}$**

Fujimura, M., <sup>a</sup>Aze, T., <sup>b</sup>Matsumura, H., <sup>c</sup>Saito, T., <sup>d</sup>Nagai, H.<sup>d</sup>, Matsuzaki,H.<sup>c</sup> (<sup>a</sup>Graduate School of Integrated Basic Sciences, Nihon University, <sup>b</sup>Graduate School of Sciences, University of Tokyo, <sup>c</sup>High Energy Accelerator Research Organization, <sup>d</sup>College of Humanities and Sciences, Nihon University, <sup>d</sup>Research Center for Nuclear Science and Technology, The University of Tokyo)

At Micro-Analysis Laboratory Tandem (MALT), the University of Tokyo, we have developed the accelerator mass spectrometry of  $^{32}\text{Si}$ ( $T_{1/2}=150-200\text{y}$ ). The chemical form of the sample was  $\text{Mg}_2\text{Si}$ , which was able to produce intense negative ion beam. The accelerator was operated at 4.5 MV, the  $5^+$  charge state was selected, and the detection of  $^{32}\text{Si}$  was carried out using the gas counter. In this paper, the state of development is described.

#### **1P22 : Comparison of MCNPX calculations with measurement results of neutron fluence in the neutrino beam line of 12GeV proton synchrotron facility at KEK**

Miura, T., Matsuda, N., Ishihama, S. (KEK)

Thermal and fast neutron fluences around the target station in the neutrino beam line of 12GeV proton synchrotron at KEK were measured using activation methods. To evaluate the Monte Carlo code, those data were compared with the calculation results by MCNPX. Calculation results were slightly larger than experimental data.

Kyusyu Univ.)

### 1P23 : Problem of neutron irradiation at the reactor for fullerene research

Sueki, K.<sup>a</sup> Endo, Y.<sup>a</sup> Akiyama, K.<sup>b</sup> Nakahara, H.<sup>c</sup> (<sup>a</sup>Graduate School of Pure and Applied Sci., Univ. of Tsukuba, <sup>b</sup>Advanced Sci. Res. Center, JAERI, <sup>c</sup>Tokyo Metro. Univ.)

The aim of this study is to investigate the stability of various fullerenes and metallofullerenes against neutron irradiation at the reactor. It is thought that there are two origins in destruction of metallofullerenes. One is recoiling nuclei due to the neutron capture reaction, and the other is radical formation due to the radiation field in the reactor. For studying the stability of metallofullerenes in the reactor, La-crude samples were irradiated at TB-tube in the JRR4. Irradiation time varied from 0 to 30 minute. It is only show that survivability of La@C<sub>82</sub> species, which was not concerned to activate the encapsulated metal atoms, was depended in the irradiation time at the reactor. However, it is show that survivability of other fullerenes and La<sub>2</sub>@C<sub>80</sub> were not changed at varied irradiation time. It is found which La@C<sub>82</sub> species to take the influence in the radiation field is different other fullerenes.

### 1P24 : Development of a synthetic method of hydrophilic endohedral <sup>133</sup>Xe-fullerenols

Watanabe, S.<sup>a</sup> Ishioka, N. S.<sup>a</sup> Sekine, T.<sup>b</sup> Kudo, H.<sup>b</sup> Shimomura, H.<sup>c</sup> Muramatsu, H.<sup>c</sup> Kume, T.<sup>a</sup> (<sup>a</sup>JAERI, <sup>b</sup>Tohoku Univ., <sup>c</sup>Faculty of Education, Shinshu Univ.)

Hydrophilic endohedral <sup>133</sup>Xe-fullerenols [<sup>133</sup>Xe@C<sub>60</sub>(OH)<sub>x</sub> and <sup>133</sup>Xe@C<sub>70</sub>(OH)<sub>x</sub>] were synthesized from hydrophobic endohedral <sup>133</sup>Xe-fullerenes. The endohedral <sup>133</sup>Xe-fullerenes dissolved in *o*-dichlorobenzene were shaken with tetrabutylammonium hydroxide and KOH solution for 1 min. On this shaking, endohedral <sup>133</sup>Xe-fullerenols formed in *o*-dichlorobenzene phase. After the shaking, the *o*-dichlorobenzene phase was separated from the KOH phase, and pure water was added to the *o*-dichlorobenzene phase. The mixture was shaken for 1 min to extract endohedral <sup>133</sup>Xe-fullerenols into pure water phase. The yield of endohedral <sup>133</sup>Xe-fullerenols, which was about 40% for C<sub>60</sub> and 23% for C<sub>70</sub>, was more than ten times as high as that obtained by using the synthetic method that we reported last year. The final products of endohedral <sup>133</sup>Xe-fullerenols in 0.9% NaCl solution were sufficiently stable for the use in nuclear medicine.

### 1P25 : Labeling of the tetradeinate N<sub>2</sub>S<sub>2</sub> ligand (MAMA) with carrier-free <sup>188</sup>Re

Hashimoto, K.<sup>a</sup> Matsuoka, H.<sup>a</sup> Ogawa, K.<sup>b,c</sup> Mukai, T.<sup>b,d</sup> Saji, H.<sup>b</sup> (<sup>a</sup>Japan Atomic Energy Res. Inst., <sup>b</sup>Kyoto Univ., <sup>c</sup>Kanazawa Univ., <sup>d</sup>

The radioisotopes of rhenium (<sup>186</sup>Re and <sup>188</sup>Re) are attractive radionuclides for radiotherapy because of their energetic beta particles and gamma rays suitable for imaging. Monoamine-monoamide dithiols (MAMA) ligands are useful in preparing radiopharmaceuticals, typically form of M(V)O(N<sub>2</sub>S<sub>2</sub>) complexes (M=Tc, Re). In this study, the labeling of MAMA ligand with carrier-free <sup>188</sup>Re from a <sup>188</sup>W/<sup>188</sup>Re generator was investigated in detail. Stannous chloride was used as a reducing agent for the reduction of rhenium and citric acid was used as a transfer ligand. The maximum labeling yields of both carrier-added and carrier-free <sup>188</sup>Re-MAMA were obtained in the acidic pH region less than pH 3 and the labeling yields decreased sharply above pH 3. Under the optimum conditions, the labeling yield of <sup>188</sup>Re-MAMA was more than 98% using carrier-free <sup>188</sup>Re as well as carrier-added <sup>188</sup>Re (20 µg Re/ml). And, both carrier-free and carrier-added <sup>188</sup>Re-MAMA were very stable in the pH 6 to 7 region during 70 hours.

### 1P26 : Preparation of platinum catalysts in microemulsions for the H<sub>2</sub>-D<sub>2</sub> isotope exchange reaction

Sakuma, N., Sugimura, E., Sawada, K., Enokida, Y., Yamamoto, I. (Graduate School of Engineering, Nagoya Univ.)

Water-in-oil microemulsions are useful system for synthesizing nanoparticles. In this study, platinum nanoparticles were prepared in water-in-oil microemulsions and deposited on diatom earth as supports at 313 K. Two kinds of microemulsions containing hexachloroplatinum acid and hydrazine in cyclohexane were prepared. The surfactant used was a nonionic surfactant tetraethyleneglycol monododecyl ether (Brij 30). Water to surfactant ratio (W) was 4. By mixing these microemulsions and the platinum ions were reduced in water core of microemulsions. The platinum nanoparticles were deposited on diatom earth supports and calcined in air at 550 °C for 1 hour. SEM analysis showed the diameter of the platinum particles prepared in microemulsions was 400-800 nm and aggregated. The H<sub>2</sub>-D<sub>2</sub> isotope exchange reaction was carried out in a stainless steel column connected to a quadrupole mass spectrometer. The HD/D<sub>2</sub> ratio was increased about 14 times as large as the original HD/D<sub>2</sub> ratio. The sample prepared in microemulsions showed catalytic activity for the H<sub>2</sub>-D<sub>2</sub> isotope exchange reaction.

### 1P27 : Application of PZC to <sup>188</sup>W/<sup>188</sup>Re generator

Matsuoka, H.<sup>a</sup> Hashimoto, K.<sup>a</sup> Hishinuma, Y.<sup>b</sup> Ishikawa, K.<sup>b</sup> Terunuma, H.<sup>b</sup> Hishinuma, K.<sup>b</sup> Uchida, S.<sup>c</sup> (<sup>a</sup>JAERI, <sup>b</sup>KAKEN, <sup>c</sup>TNS)

Rhenium-188 is an attractive radionuclide for radiotherapy and can

be obtained at carrier-free levels from a  $^{188}\text{W}/^{188}\text{Re}$  generator. The concentration of  $^{188}\text{Re}$  is relatively low from traditional alumina-based  $^{188}\text{W}/^{188}\text{Re}$  generators, because the parent  $^{188}\text{W}$  is produced in a relatively low specific activity by the double neutron capture reaction of enriched  $^{186}\text{W}$ . Newly developed poly zirconium compound (PZC) as the adsorbent of  $^{99}\text{Mo}$  has more than 100 times higher adsorption capacity of molybdenum than alumina. In this study, applicability of PZC to an adsorbent for a  $^{188}\text{W}/^{188}\text{Re}$  generator system was investigated. The PZC generator gave reproducible  $^{188}\text{Re}$  elution yields (over 60%) with low  $^{188}\text{W}$  parent breakthrough (0.03%) during 154 days corresponding to twice of the half-life of  $^{188}\text{W}$  (69.4 day). The labeling yields of hydroxyethyliden diphosphonic acid (HEDP) and mercaptoacetyltriglycine (MAG3) with  $^{188}\text{Re}$  eluted from the PZC column were high enough and equal to the results using  $^{188}\text{Re}$  eluted from the alumina system.

#### **1P28 : A new method of producing multitracer by using a liquid catcher and the chemical effect of the catcher yields**

Yatsukawa, M., <sup>a</sup> Kasamatsu, Y., <sup>a</sup> Kikunaga, H., <sup>b</sup> Kinoshita, N., <sup>b</sup> Hashimoto, T., <sup>b</sup> Arai, M., <sup>b</sup> Ninomiya, K., <sup>a</sup> Yokoyama, A., <sup>b</sup> Sato, W., <sup>a</sup> Takahashi, N., <sup>a</sup> Shibata, S., <sup>c</sup> Shinohara, A. <sup>a</sup> (<sup>a</sup>Grad. School Sci., Osaka Univ., <sup>b</sup>Grad. School Natural Sci., Kanazawa Univ., <sup>c</sup>Nuclear Safety Technology Center)

Recently, the multitracer technique is useful in various fields. For the online production of a multitracer solution, we have developed a new target system, by which the recoil products are directly introduced into solvent and then transported through a tube from the irradiation chamber to a solution reservoir. After the irradiation, we measured the radioactivities in the solution with Ge-detectors and determined the yields of them. The yields were defined as the relative values to those for the stacked catcher foils. It was found that the values depend on pH of the solution.

#### **1P29 : Hydrogen isotopes separation effect by electrolysis using solid polymer electrolyte**

Ogata, Y., <sup>a</sup> Sakuma, Y., <sup>b</sup> Ohtani, N., <sup>c</sup> Kotaka, M., <sup>d</sup> (<sup>a</sup>Nagoya Univ., <sup>b</sup>NIFS, <sup>c</sup>Wakasawan Energy Res., <sup>d</sup>Theoretical Radiation Res.)

Hydrogen isotope separation effect by electrolysis of water was theoretically investigated and was compared with experimental results. The separation mechanism was analyzed as the hydrogen isotope exchange reaction between water and diatomic hydride that consists of hydrogen and cathode material. The equilibrium constants of the isotope exchange reaction were calculated from reduced partition function ratio. Using the constants, the separation factor (*SF*) of the

isotopes was calculated according to the two-phase distribution theory for isotopes. On the other hand, light or heavy water spiked with tritiated water was electrolyzed with a device using a solid polymer electrolyte, which equipped with SUS, Ni, or carbon cathode. Thus, the *SFs* were experimentally obtained. Calculated *SFs* were well agreed with the experimentally values for SUS or Ni cathode, and that for carbon cathode was somewhat small than the experimental value.

#### **1P30 : Positron annihilation processes in supercritical fluids of $\text{CO}_2$ and $\text{N}_2\text{O}$**

Funakoshi, K., <sup>a</sup> Kino, Y., <sup>a</sup> Sekine, T., <sup>a</sup> Kudo, H., <sup>a</sup> Suzuki, T., <sup>b</sup> Ito, Y. <sup>b</sup> (<sup>a</sup>Tohoku Univ., <sup>b</sup>KEK)

We measured positron annihilation lifetime (PAL) spectra in  $\text{N}_2\text{O}$  and  $\text{CO}_2$ , focusing on density dependence in the medium including the supercritical fluid phase, in the range from  $1 \text{ nm}^{-3}$  to  $13 \text{ nm}^{-3}$ . The PAL spectra were resolved into four components using the PATFIT code. We found the formation of two types of *o*-Ps in  $\text{N}_2\text{O}$ . The longest lifetime component was attributed to the *o*-Ps pick-off annihilation that was observed continuously from the gaseous phase to the liquid phase, and the third lifetime component (the second longest) appeared in the density higher than  $4.5 \text{ nm}^{-3}$ . The result strongly suggests the existence of different annihilation circumstances for the *o*-Ps pick-off processes in dense  $\text{N}_2\text{O}$ . The longest lifetime component was also observed in  $\text{CO}_2$  as in the case of  $\text{N}_2\text{O}$ , while the third component did not appear in  $\text{CO}_2$ .

#### **1P31 : Electronic structure of hydrated $\text{No}^{2+}$ ion**

Hirata, M., <sup>a</sup> Nagame, Y., <sup>a</sup> Anton, J., <sup>b</sup> Fricke, B., <sup>b</sup> (<sup>a</sup>Japan Atomic Energy Research Institute, <sup>b</sup>Kassel University)

We performed relativistic density functional calculations to estimate the stability of  $\text{No}^{2+}$  ion in solution. First we optimized interatomic distances between the cation and oxygen of water molecules by the relativistic LDA. Next, we precisely calculated their binding energy of hydration by noncollinear RDFT program with several exchange/correlation functionals. The ionic radius of  $\text{No}^{2+}$  is similar to  $\text{Ca}^{2+}$  ion.

#### **1P32 : The interaction between trivalent 4f and 5f-block elements and thiocyanate ion**

Mori, T., Suganuma, H., Yanaga, M. (Radiochem. Res. Lab., Fac. of Sci., Shizuoka Univ.), Satoh, I. (IMR, Tohoku Univ.)

The formation constants of thiocyanate complexes of Eu(III), <sup>152,154</sup>Eu, and Am(III), <sup>241</sup>Am, in trace concentrations were investigated in mixed solvent ( $\text{CH}_3\text{OH} + \text{H}_2\text{O}$ ) solutions of different ionic strength. The formation constant was obtained by a back-extraction technique.

The results showed that the formation constants of thiocyanate complexes of Eu(III) and Am(III) were approximately same values in 1.0 M (H, Na)(SCN, ClO<sub>4</sub>) + 5.0 M LiCl aqueous solution, but the formation constant of thiocyanate complex of Am(III) was considerably larger than that of Eu(III) in 1.0 M(H, Na)(SCN, ClO<sub>4</sub>) mixed solvent solution ( $X_{\text{MeOH}} = 0.40$ ). Furthermore, in paper electrophoresis, the migration velocities of the species of Eu(III) and Am(III) were investigated in 1.1 M(H, Na)(SCN, ClO<sub>4</sub>) aqueous solutions. The results showed that the migration velocities of Eu(III) and Am(III) were decreased with an increase in the concentration of SCN<sup>-</sup>.

### 1P33 : Solvent extraction of f-block element ions with thiocalix[4]arenes and their oxides (2)

Matsuyama, K., Yanaga, M., Irikawa, H.<sup>1</sup>, Satoh, I.<sup>2</sup>, Saganuma, H. (Radiochem. Res. Lab., Shizuoka Univ., <sup>1</sup>Fac. Sci, Shizuoka Univ., <sup>2</sup>IMR, Tohoku Univ.)

It is expected that thiocalix[4]arenes and their oxides (sulfinyl- and sulfonylcalix[4]arenes) have the ability of selective complexation for metal ions, based on HSAB principle. We synthesised thiocalix[4]arenes and their oxides from two kinds of *p*-alkylphenol (*p*-*tert*-butyl- and *p*-*tert*-octylphenol). The extraction behaviors of <sup>152</sup>Eu(III) and <sup>241</sup>Am(III) in the solution of pH region of 4~6.2 were investigated using those extractants dissolved into chloroform and their distribution ratios were calculated ( $D = [M^{3+}]_{\text{org}}/[M^{3+}]_{\text{aq}}$ ). Both metal ions were extracted by those extractants in a following order; sulfinyl- > sulfonyl- > thiocalix[4]arene. The sulfinyl- and sulfonyl compounds showed efficiently extraction for both elements, but this compounds showed poor extractability. When sodium perchlorate was added to aqueous phase (pH= 5.3), the sulfinyl compound had an enlarging difference between  $D$  values of both metals with an increase in perchlorate concentration (Eu(III) was more extracted than Am(III)).

### 1P34 : Study on Separation of Trivalent Actinide Ion from Trivalent Lanthanide Ion using Chitosan Derivatives

Miyashita.I.S.<sup>1</sup>, Irikawa.H.<sup>2</sup>, Satoh.I.<sup>3</sup>, Yanaga.M.<sup>1</sup>, Saganuma.H.<sup>1</sup> (Radiochem. Res. Lab., Fac. of Sci., Shizuoka Univ.<sup>1</sup>, Dept. Chem. Fac., of Sci., Shizuoka Univ.<sup>2</sup>, IMR, Tohoku Univ.<sup>3</sup>)

The extraction behaviors of <sup>152,154</sup>Eu(III) and <sup>241</sup>Am(III) using dithiocarbamate lipophilic chitosan(DTCLC) were investigated. It was found that distribution ratios of Am(III) in the region of 4<pH<6.5 is higher than that of Eu(III) when the aqueous phase contains 0.1 M sodium perchlorate and the slopes of log $D$  vs pH are about +1. The distribution ratios of Eu(III) and Am(III) are increased with increasing the ligand concentration dissolved in chloroform. The slopes of log $D$  vs DTCLC concentration in chloroform on Eu(III) and Am(III) are +1 and

+2, respectively. With an increase of sodium perchlorate concentration from 1 M to 3 M in aqueous solution, the distribution ratios of Eu(III) and Am(III) are increased and the slopes of log $D$  vs log[ClO<sub>4</sub><sup>-</sup>] are about +2. However, in the concentration region of ClO<sub>4</sub><sup>-</sup>, a significant difference between the distribution ratios of Eu(III) and Am(III) were not found.

### 1P35 : Study of separation mechanism of actinide and lanthanide with diglycolamide by SANS and EXAFS

Yaita, T.<sup>a</sup>, Narita, H.<sup>b</sup>, Kimura, T.<sup>a</sup>, Jensen, M. P.<sup>c</sup> (JAERI<sup>a</sup>, AIST<sup>b</sup>, ANL<sup>c</sup>)

Separation mechanism of trivalent actinide (An<sup>3+</sup>) and lanthanide (Ln<sup>3+</sup>) with diglycolamide (DGA) was clarified by EXAFS and SANS. DGA is one of the best ligands in the separation reagents of An<sup>3+</sup> and Ln<sup>3+</sup>. X-ray crystallography and EXAFS data demonstrates that DGA coordinates stably to the ions with semi-tridentate and tridentate fashion. Therefore, the local structure of complex with An<sup>3+</sup> and Ln<sup>3+</sup> does not change significantly in an extraction from concentrated nitric acid solution. From the view points of aggregation properties of DGA determined by SANS, however, there are clear differences in the aggregation structure between 1M and 2M extraction. Thus, DGA exists as monomer or dimer below 1M HNO<sub>3</sub>; DGA forms (DGA)<sub>6</sub> above 2M HNO<sub>3</sub>. The forming hexamer would relate with the extraction of An<sup>3+</sup> and Ln<sup>3+</sup> above 2M HNO<sub>3</sub>, since the extraction efficiency of An<sup>3+</sup> and Ln<sup>3+</sup> above 2M HNO<sub>3</sub> increases drastically.

### 1P36 : Decontamination of radioactive corrosion products utilizing water-in-CO<sub>2</sub> reversed micelles

Shimizu, R., Sawada, K., Enokida, Y., Yamamoto, I. (Department of Materials, Physics and Energy Engineering, Nagoya Univ.)

Decontamination of magnetite (Fe<sub>3</sub>O<sub>4</sub>) utilizing water-in-CO<sub>2</sub> reversed micelles was performed. Magnetite is main oxide deposited on the primary heat transport impregnated with active Co<sup>2+</sup> and fission products. CO<sub>2</sub> is one of the most environmentally benign and practical solvent because of its non-toxic, non-flammable, and inexpensive nature. Pentadecafluorooctanoic acid (PFOA), which has carboxyl group, was used as a surfactant. Black shots (High Purity Chemicals) which were iron spheres covered by magnetite were used as test specimens. About 400 mg of black shots were placed in a stainless steel column. A 0.1 cm<sup>3</sup> of water and 1.05 wt% of PFOA were mixed with CO<sub>2</sub> at 16 MPa, 323 K in a high-pressure cell (60 cm<sup>3</sup>). Well-mixed CO<sub>2</sub>/PFOA/H<sub>2</sub>O was introduced from the cell to the column. Decontamination was conducted under the static condition for 1 h and dynamic condition for 3 h. Ultrasound was irradiated to the column through the experiment. It was observed that the surface of black shots

was metallic luster attributed to the detachment of magnetite. The decrease of black shots was 2.1 mg.

**1P37 : Olfactory transport of alkaline metal ions by intranasal administration (2) -Uptake behavior of  $^{24}\text{Na}^+$  and  $^{43}\text{K}^+$ -**

Kanayama, Y.<sup>1</sup> Hirunuma, R.<sup>2</sup> Haba, H.<sup>2</sup> Enomoto, S.<sup>2</sup> Amano, R.<sup>1</sup> (Kanazawa Univ.,<sup>1</sup> RIKEN<sup>2</sup>)

Olfactory axonal transport provides direct transport of variable solutes from the nasal cavity to the brain. In our previous studies, we demonstrated that  $\text{Rb}^+$ ,  $\text{Cs}^+$ , and  $\text{TI}^+$ , which are  $\text{K}^+$ -mimic ions, are unilaterally accumulated and transported to the olfactory bulb and cortex after unilateral intranasal administration. These ions are transported via the olfactory pathway, however, underlying mechanisms and physiological roles of the axonal transport of the  $\text{K}^+$ -mimic ions are poorly understood. Thus we attempted to use the multitracer from Ti target, which enables simultaneous tracing of  $^{24}\text{Na}^+$ ,  $^{28}\text{Mg}^{2+}$ ,  $^{43}\text{K}^+$ , and  $^{47}\text{Ca}^{2+}$  for clarifying their olfactory transport. Following intranasal administration of the multitracer, the  $^{43}\text{K}^+$  uptake rates in the olfactory bulb showed the highest level in the brain regions. Furthermore, the high level of  $^{28}\text{Mg}^{2+}$  was also observed in the olfactory bulbs. In contrast, the  $^{24}\text{Na}^+$  showed low uptake rates in the whole brain regions. The results indicate that  $\text{Mg}^{2+}$  and  $\text{K}^+$  are directly transported from the nostril to the brain via the olfactory pathway.

**1P38 : Excretion rate of biotrace elements in bile of rat under oxidative stress of Se-deficiency**

Endo, K.<sup>1</sup> Yamazaki, K.<sup>2</sup> Matsumoto, K.<sup>3</sup> Tsukada, M.<sup>2</sup> Hondao, C.<sup>1</sup> Matsuoka, K.<sup>1</sup> Hirayama, R.<sup>4</sup> Enomoto, S.<sup>4</sup> (Showa Pharm Univ<sup>1</sup>, Meiji Univ<sup>2</sup>, NIH<sup>3</sup>, RIKEN<sup>4</sup>)

It is known that biological organs are exposed to oxidative stress under Se-deficient conditions. The oxidative stress will change the distributions of bio-trace elements in organs to keep mineral-balance. Metabolism in liver plays important roles for the homeostasis of trace elements. In this work, the excretion rates of bio-trace elements in bile of Se-deficient and normal rats were examined using multi-tracer (MT) technique. Zn and Fe were not detected both in bile of Se-deficient and normal rats for 60 min after intravenous (i.v.) administration of multitracer, while the excretion rates of Sr, As, Mn, Co, and V reached plateau mostly up to 20 min after the MT administration. The excretion rate of Se in Se-deficient rat was about 1/5 slower than in normal rat. The results will be presented in connection with the role of each metal ion in animal.

**1P39 : Syntheses of Re-186 and Re-188-labelled**

**radiopharmaceuticals in organic solvents**

Nogawa, N., Ooshiro, S., Yamaguti, T., Makide, Y., Morikawa, N.,<sup>a</sup> Matuoka, H.,<sup>a</sup> Hashimoto, K.,<sup>a</sup> Sato, A. (Radioisotope Center, The University of Tokyo, <sup>a</sup>JAERI)

Re-186 and Re-188 are expected to be effective for pain palliation of skeletal metastases and cancer therapy. Syntheses condition of Re-186 and Re-188-labelled radiopharmaceuticals requires a larger quantity of  $\text{SnCl}_2$ , lower pH of solution, higher temperature and longer reaction time in comparison with that of  $\text{Tc-99m}$ -labelled radiopharmaceuticals. The effect on the reaction yield of organic solvents which increase  $[\text{Cl}^-] / [\text{OH}^-]$  by adding small quantity of HCl or  $\text{SnCl}_2$  was examined in order to attain milder and more convenient conditions. Reaction between  $^{186}\text{ReO}_4^-$  solution or  $^{188}\text{ReO}_4^-$  eluted from  $^{188}\text{W}/^{188}\text{Re}$  generator both and HEDP or DMSA was studied. MeOH, EtOH, 1-Butanol or 1-Octanol was used as a solvent. When the organic solvent was used as the solvent instead of the water, the reaction yield increased under the milder conditions. The reactivity of Re seems to be accelerated by the coordination of  $\text{Cl}^-$  instead of  $\text{OH}^-$  in Re ions.

**1P40 : Calculation of the reaction rate constant of DNA base with the hydroxyl radical studied by the rapid flow-ESR method**

Taguchi, H.<sup>1</sup>, Takeuchi, Y.<sup>1</sup>, Yoshioka, H.<sup>2</sup>, Yoshioka, H.<sup>1</sup> (<sup>1</sup>Radiochem. Res. Lab., Fac. of Sci., Shizuoka Univ., <sup>2</sup>Inst. for Environmental Sci., Univ. of Shizuoka)

It is possible to measure the ESR spectra of short-lived radicals by the rapid flow-ESR method. We have already studied about deoxyribose and DNA base radicals formed by the reaction with the hydroxyl radical ( $\cdot\text{OH}$ ) using this method. It is also possible to obtain reaction rate constants of antioxidant molecules with  $\cdot\text{OH}$ . In this case, a competitive reaction between the antioxidant and a standard molecule with  $\cdot\text{OH}$  is employed. In addition, it is required that side reaction does not occur in this system. We aimed to obtain the reaction rate constant of DNA base with  $\cdot\text{OH}$  using this method. When alcohols were used as the standard, a side reaction between the radicals derived from alcohols and the base happened and it made analysis of the spectrum impossible. In this report, polyphenols were used instead of alcohols and, as a result, a reasonable result was obtained.

**1P41 : Quantum-chemical analysis of the reaction rate constants of polyphenols with hydroxyl radical**

Takeuchi, Y.<sup>a</sup> Taguchi, H.<sup>a</sup> Hirama, M.,<sup>b</sup> Yoshioka, H.,<sup>c</sup> Yoshioka, H.<sup>a</sup> (<sup>a</sup> Radiochem. Res. Lab., Fac. of Sci., Shizuoka Univ., <sup>b</sup> Fac. of Sci., Shizuoka Univ., <sup>c</sup> Inst. for Env. Sci., Univ. of Shizuoka)

ESR spectra of the antioxidant radical formed by the reaction with the hydroxyl radical ( $\cdot\text{OH}$ ) generated from  $\text{Ti}^{3+} + \text{H}_2\text{O}_2$  system was measured using the rapid flow method. When the mixture of an antioxidant and ethanol was reacted with  $\cdot\text{OH}$ , a superposed spectrum of the 1-hydroxyethyl radical and of the antioxidant radical was measured. The intensity ratio of signals of these radicals was calculated from the doubly-integrated curve, and the ratio of the second order reaction rate constant of the antioxidant with  $\cdot\text{OH}$  to that of ethanol was obtained. Bond dissociation energies (BDEs) of the reactive sites in antioxidant molecules were obtained by quantum-chemical calculation. Relationship between the relative activation energies obtained from rate constants and the BDEs showed that Evans-Polanyi equation holds in polyphenol series but the values of alcohols shift from the line.

#### 1P42 : Estimation of measurement precision based on FUMI theory in HPLC analysis for radiopharmaceuticals

Kitajima, A.<sup>a</sup> Tazawa, S.<sup>a</sup> Hatsushiba, K.,<sup>a</sup> Minamizawa, T.,<sup>a</sup> Matsuda, R.,<sup>b</sup> Hayashi, Y.<sup>b</sup> (<sup>a</sup>Daiichi Radioisotope Lab., <sup>b</sup>National Institute of Health Sciences)

The method validation requires the exact description of precision of the test method. Usually, the standard deviation of measurements is calculated from repeated experiments. However, there is serious problem in case of the analysis for the short half-life compounds labeled by  $^{123}\text{I}$ ,  $^{99m}\text{Tc}$ ,  $^{18}\text{F}$ , and so on. The HPLC peak decreases during the period of the repeated experiments according to its half-life. That is, the SD cannot be defined based on the peak area that is not reproducible within experimental errors. Now, we are trying to solve the above problem by a method called FUMI theory that enables the SD estimation from the stochastic properties of noise and signal in the instrumental output. Precision profile at Fig.1 was obtained from the repeated ( $n=6$ ) experiments with the short measurement time (2min.) which requires no half-life correction. The profile shows the good agreement between the predicted RSD by FUMI theory and the observed one, indicating the applicability of the FUMI theory to HPLC equipped with RI detector.

#### 2A01 : Elucidation of methane generation process in stainless steel surface using tritium

Higaki, S., Oya, Y., Makide, Y. (Radioisotope Center, The Univ. of Tokyo)

Although it is known that methane is emitted from stainless steel (SS) by the metal-metal collision or deformation, its process and mechanism has not been studied at all. In this work, after making tritium gas ( $\text{T}_2$  in  $\text{D}_2$ ) permeated inside SS canister containing many small SS balls at high temperature, the canister was evacuated, and then shaken

under the helium atmosphere. After the emitted tritium and methane were collected once with molecular sieves at low temperature, they were separated and determined with a radio-gas chromatograph equipped with an FID for  $\text{CH}_4$  and a proportional counter for HT and  $\text{CH}_3\text{T}$  detection. The generation and release of  $\text{CH}_4$  and  $\text{CH}_3\text{T}$  were studied in various conditions, and were compared with the behavior of HT. The release of  $\text{CH}_4$  and  $\text{CH}_3\text{T}$  was found only by shaking the canister with SS balls.

#### 2A02 : Mass and temperature dependences of isotope effects in U(IV)/U(VI) exchange equilibrium reaction

Nomura M., Suzuki T., Fujii Y. (Research Lab. Nucl. Reactors, Tokyo Inst. Technol.)

Isotope effects in the equilibrium between U(IV) and U(VI) ions have been studied at high temperatures. To determine the effects, chromatographic isotope separation experiments were conducted by using strongly basic, high porous anion exchange resin. The adsorbed U(VI) ions were eluted with an reducing reagent of V(III) and the eluted U(IV) ions were again oxidized to U(VI) by Fe(III) ions initially adsorbed in the resin. Thus uranium adsorption band was migrated in a displacement chromatography between the zones of oxidizing reagent and reducing reagent ca. 4 m. The chromatographic operations were conducted at different temperatures of 87, 100, 120, 140, 160 °C. The effluents were collected in fractions and subjected to concentration and isotope abundance analyses. The results gave the isotopic equilibrium constants of U(IV)-U(VI) exchange reaction. The determined isotope equilibrium constants are discussed in comparing with the theory for the field shift isotope effects recently formulated by Bigeleisen.

#### 2A03 : Phenoxo bridged dimeric structure of technetium(I) tricarbonyl complex with Schiff base ligand

Harano, A., Takayama, T., Sekine, T., Kudo, H. (Tohoku Univ.)

A novel tricarbonyl technetium(I) complexe with Schiff base ligand  $[\text{Tc}(\text{CO})_3(\text{salbut})]_2$  was synthesized from the reaction of  $(\text{Et}_4\text{N})_2[\text{TcCl}_3(\text{CO})_3]$  and Hsalbut with  $\text{NEt}_3$ . Addition of base is necessary for formation of  $[\text{Tc}(\text{CO})_3(\text{salbut})]_2$  in this reaction. Yellow plate single crystals of  $[\text{Tc}(\text{CO})_3(\text{salbut})]_2$  were obtained by recrystallization from benzene solution. X-ray crystal structure analysis for these crystals shows the phenoxo bridged dimeric structure of  $[\text{Tc}(\text{CO})_3(\text{salbut})]_2$ . An anionic ligand (salbut)<sup>-</sup> bounds to the technetium atom with nitrogen and oxygen atoms as a bidentate ligand. Three carbonyl ligands coordinated to the technetium atom are in the facial form. The Tc-O-Tc bridging bond is formed by donation of two unshared electron pairs on the anionic oxygen atom of phenoxy groups to technetium atoms.

**2A04 : Substituent and solvent effects on the *syn*-to-*anti* formation ratio of nitrido technetium(V) complexes with salen type bifunctional ligands**

Yuse, K., Takayama, T., Sekine, T., Kudo, H. (Graduate School of Sci., Tohoku Univ.)

The reaction of  $\text{TcNCl}_2(\text{PPh}_3)_2$  and salen type ligands with a substituent in the bridging alkyl group was investigated in  $\text{CH}_2\text{Cl}_2$  and DMSO solvents. The *syn*-to-*anti* formation ratio of the complexes obtained is discussed. The ratio is mainly affected by the steric hindrance in  $\text{CH}_2\text{Cl}_2$ . In DMSO, on the other hand, the polarity of substituents would play a role in determining the ratio.

**2B01 : Inhibiting effect of tea catechin on the lipid peroxidation induced in tritiated water**

Kubota, M., <sup>a</sup> Takeuchi, Y., <sup>a</sup> Okuno, K., <sup>a</sup> Yoshioka, H., <sup>b</sup> and Yoshioka, H. <sup>a</sup> (<sup>a</sup> Radiochem. Res. Lab., Fac. of Sci., Shizuoka Univ., <sup>b</sup> Inst. For Env. Sci., Univ. of Shizuoka)

Lipid peroxidation in biomembranes damages bio-organisms like the case of DNA scission. We have studied the inhibiting effect of tea catechins on the lipid peroxidation induced by  $^{60}\text{Co}$   $\gamma$ -ray. In this report, the peroxidation induced by  $\beta$ -ray in tritiated water and the inhibiting effect were examined focusing attention especially on the temperature dependency of the reaction rate, because accurate temperature regulation was possible in contrast to the case of  $\gamma$ -ray experiment. Peroxidation rate increased with elevating temperature in both cases with and without tea catechin, (-)-epigallocatechin gallate (EGCg). But, EGCg showed the inhibiting effect on  $\beta$ -ray induced lipid peroxidation.

**2B02 : Study of boron in plants using Doppler broadening of prompt  $\gamma$ -rays**

Sakai, Y., <sup>a</sup> Kubo, M. K., <sup>b</sup> Matsue, H., <sup>c</sup> Matsunaga, T., <sup>d</sup> Yonezawa, C. <sup>c</sup> (<sup>a</sup>Daido Inst. Tech., <sup>b</sup>Intern. Christ. Univ., <sup>c</sup>JAERI, <sup>d</sup>KONARC, <sup>e</sup>IAEA)

By probing Doppler broadened line-shapes of prompt  $\gamma$ -ray at 478 keV emitted from moving  $^7\text{Li}$  produced via the  $^{10}\text{B}(\text{n},\alpha)^7\text{Li}$  reaction, matrix materials containing and/or surrounding boron species were non-destructively characterized for several plants such as soybeans and apples. Prompt  $\gamma$ -ray measurements were carried out at the PGA set-up installed in JRR-3M of Japan Atomic Energy Research Institute. It was demonstrated that boron species should exist in an aqueous solution for fresh apple fruit, while boron in dried apple fruit be surrounded by denser matrix materials.

**2B03 : Analysis of the radionuclides induced in a medical cyclotron and the radioactive by-products in radiopharmaceuticals for positron emission tomography (PET)**

Mochizuki, S., Ogata, Y., Hatano, K. <sup>1</sup>, Abe, J. <sup>1</sup>, Ito, K. <sup>1</sup>, Nishino, M. <sup>2</sup>, Miyahara, H. (Graduate School of Medicine, Nagoya Univ., National Inst. for Longevity Sci. <sup>1</sup>, Nagoya Univ. Hospital <sup>2</sup>)

A medical cyclotron is activated itself in the producing process of radiopharmaceuticals for positron emission tomography (PET) and radioactive by-products were induced in target materials. Some problems may arise in the radiation exposure to the staff and radioactive waste administration. The radioactive by-products may be contained in the PET radiopharmaceuticals; therefore, we examined the exchanged parts, PET radiopharmaceuticals, and columns used for PET radiopharmaceuticals synthesis. Measurements were carried out using a high-purity germanium gamma-ray detector for all samples and using a liquid scintillation counter for tritium in enriched [ $^{18}\text{O}$ ] water and [ $^{18}\text{F}$ ]-FDG solution. Radionuclides of  $^{22}\text{Na}$ ,  $^{46}\text{Sc}$ ,  $^{48}\text{V}$ ,  $^{51}\text{Cr}$ ,  $^{52}\text{Mn}$ ,  $^{54}\text{Mn}$ ,  $^{56}\text{Co}$ ,  $^{57}\text{Co}$ ,  $^{58}\text{Co}$ ,  $^{60}\text{Co}$ ,  $^{65}\text{Zn}$ ,  $^{95m}\text{Tc}$ ,  $^{96}\text{Tc}$ , and  $^{184}\text{Re}$  were found in the target windows used for production of  $^{11}\text{C}$ ,  $^{15}\text{O}$ ,  $^{18}\text{F}$ , and tritium was detected in both [ $^{18}\text{O}$ ] water after irradiation and after distillation. However, radionuclide except for  $^{18}\text{F}$  was not recognized in [ $^{18}\text{F}$ ]-FDG produced by the  $^{18}\text{O}(\text{p}, \text{n})^{18}\text{F}$  reaction.

**2B04 : Biodistribution of  $^{224}\text{Ra}$  and  $^{223}\text{Ra}$  and retention of its progeny nuclides,  $^{212}\text{Pb}$  and  $^{211}\text{Pb}$**

Washiyama, K. <sup>a</sup>, Sasaki, J. <sup>a</sup>, Ogawa, D. <sup>a</sup>, Mitsugashira, T. <sup>b</sup>, Amano, R. <sup>a</sup> (<sup>a</sup>Fac. Med., Kanazawa Univ., Institute for Material Research, Tohoku Univ.)

Our previous study of the biodistribution of  $^{227}\text{Th}$ -EDTMP for bone metastases agent demonstrated significant skeletal accumulation and high retention rate of daughter nuclide  $^{223}\text{Ra}$  in bone. In this work the biodistribution of  $^{223}\text{Ra}$  and the retention of its progeny in bone were evaluated. We also measured the biodistribution of  $^{224}\text{Ra}$  and its daughter  $^{212}\text{Pb}$  skeletal retention to compare the effect of the half-life of noble gas element Rn in both decay series.

Each Ra isotope was injected into different ICR, 8-week-old, male mice and dissected at several time points. Femur and several tissues were excised and subjected to  $\gamma$ -ray spectrometry.

Three hours, 3 days and 7 days after injection of  $^{223}\text{Ra}$  the skeletal retentions of  $^{211}\text{Pb}$  were 68.7%, 78.7% and 82.7%, respectively. And of  $^{212}\text{Pb}$  2days after  $^{224}\text{Ra}$  injection was 39.1%. The difference in Pb retention between two decay series reflected the half-life of noble gas nuclides,  $^{209}\text{Rn}$  and  $^{210}\text{Rn}$ . The increase of the skeletal retention of  $^{211}\text{Pb}$

during 7days reflected Ra mineralization into bone volume.

## 2P01 : Atomic Number Dependence of the Energy Shifts of Electronic X rays from Pionic Atoms

H. Sugiura<sup>1</sup>, K. Ninomiya<sup>1</sup>, Y. Kasamatsu<sup>1</sup>, H. Kikunaga<sup>2</sup>, N. Kinoshita<sup>2</sup>, Y. Tani<sup>1</sup>, H. Hasegawa<sup>1</sup>, M. Yatsukawa<sup>1</sup>, K. Takamiya<sup>3</sup>, H. Matsumura<sup>4</sup>, W. Sato<sup>1</sup>, T. Yoshimura<sup>1</sup>, A. Yokoyama<sup>5</sup>, K. Sueki<sup>6</sup>, Y. Hamajima<sup>7</sup>, T. Miura<sup>4</sup> and A. Shinohara<sup>1</sup> (<sup>1</sup>Grad School Sci Osaka Univ., <sup>2</sup>Grad School Natural Sci Kanazawa Univ., <sup>3</sup>Res. Reactor Inst., Kyoto Univ., <sup>4</sup>Res. Center Radiation, KEK., <sup>5</sup> Faculty Sci., Kanazawa Univ., <sup>6</sup>Dept. Chem., Univ. Tsukuba, <sup>7</sup>LLRL, Inst. Nature and Env. Technol., Kanazawa Univ.)

Pionic X rays and electronic X rays were measured for pionic atoms of 11 elements, to reveal the electron rearrangement during the pion cascade. The energy differences were observed between the electronic X rays of pionic Z atoms (Z:the atomic number) and those of (Z-1) atoms. The atomic states after the formation of the pionic atoms will be discussed on the basis of the atomic number dependence of the energy difference.

## 2P02 : Detection of short-lived cosmogenic nuclides in rainwater

Kuwahara, Y.<sup>a</sup>, Tanaka, K.<sup>b</sup>, Murata, Y.<sup>c</sup>, Inoue, M.<sup>c</sup>, Komura, K.<sup>c</sup>  
(<sup>a</sup>Graduated School of Natural Sci. and Technol. Kanazawa Univ.,  
<sup>b</sup>Faculty Sci., Kanazawa Univ., <sup>c</sup>K-INET ,Kanazawa Univ.)

We tried to detect short-lived cosmogenic radionuclides in freshly precipitated rainwater. About 30-50L of rainwater was collected through downpour from the roof of our laboratory. Cosmogenic radionuclides were swiftly separated by using anion and cation type POWDEX-PAO and POWDEX-PCH resin and measured by ultra-low background Ge detector in Ogoya Underground Laboratory. Short-lived nuclides detected are <sup>24</sup>Na (half-life 14.96 h), <sup>28</sup>Mg (20.91 h), <sup>38</sup>S (170.3 m), <sup>38</sup>Cl (37.24 m) and <sup>39</sup>Cl (55.6 m). Activity levels and activity ratios of these nuclides relative to <sup>7</sup>Be (53.3 d) will be discussed

## 2P03 : Estimating growth rate of hokutolite from Tamagawa hot spring

Saito, T., Nagai, H. (College of Humanities & Sciences, Nihon Univ.)

The concentrations of radium isotopes and the progenies (<sup>226</sup>Ra, <sup>228</sup>Ra and <sup>228</sup>Th) in three hokutolite samples from Tamagawa hot spring were measured. These isotopes were analyzed by a well-type HPGe  $\gamma$ -ray spectrometer for the 351, 609, 911 and 583 keV  $\gamma$ -ray from <sup>214</sup>Pb, <sup>214</sup>Bi, <sup>228</sup>Ac and <sup>208</sup>Tl, respectively, each being in radioactive equilibrium with precursors. The <sup>226</sup>Ra concentrations are in the range

of 50-85 Bq/g, being higher in the lower layer. The <sup>228</sup>Ra concentrations are in the range of 7.1-263 Bq/g, being higher in the upper layer. The activity ratios of <sup>228</sup>Ra/<sup>226</sup>Ra provided the estimation of the growth rate (0.06 - 0.20 mm/y). These estimated growth rate were correlated with SO<sub>4</sub><sup>2-</sup> concentration in Tamagawa hot spring water. Estimated <sup>228</sup>Ra/<sup>226</sup>Ra activity ratios in Tamagawa hot spring water from hokutolite surface activity were concordant with the actual hot spring water.

## 2P04 : Behavior of uranium series nuclides in core samples in Kanamaru area, Yamagata Prefecture

Kanai, Y., Kamioka, H., Seki, Y., Naito, K. and Watanabe, Y. (AIST, Geological Survey of Japan)

In order to elucidate the movement-retention behavior of uranium in the sediment, uranium in the boring core and groundwater in the Kanamaru area, Yamagata Prefecture, was studied. Two boring cores of 37.5m and 30.0m length were obtained. Uranium was rich in the core of 10-12 m depth from the surface. The maximum content was about 2500ppm. The groundwaters in the borehole were taken from about 10m and 20m depth. The uranium content in the shallow groundwater (0.2ppb; -10m depth) was lower than the deeper one (1.4ppb; -20m depth). The uranium series nuclides such as U-238, U-234 and Th-230 in the core and groundwater were determined. Most of the core samples from 10-12m depth have U-234/U-238 activity ratios of >1 and Th-230/U-234 <1, suggesting the U accumulation. On the other hand, the shallow groundwater (-10m depth) has U-234/U-238 activity ratios of >1 and Th-230/U-234 >1, while the deeper one (-20m depth) has U-234/U-238 activity ratios of >1 and Th-230/U-234 <1. From these results, it is supposed that U is adsorbed on the sediment from groundwater at 10m depth.

## 2P05 : Mössbauer Study of (Sr,Ca)RuO<sub>3</sub><sub>δ</sub> doped with <sup>57</sup>Fe

Kiyoshi Nomura<sup>1</sup>, Radek Zboril<sup>2</sup>, Miloslav Mashlan<sup>2</sup>, Alexandre Rykov<sup>1</sup>, Israel Felner<sup>3</sup> (<sup>1</sup>School of Engineering, The University of Tokyo, <sup>2</sup>Departments of Physical Chemistry and Experimental Physics, Palacky University, <sup>3</sup>The Racah Institute of Physics, The Hebrew University of Jerusalem)

Felner et al [1] showed that T<sub>C</sub> of CaRu<sub>1-x</sub>Fe<sub>x</sub>O<sub>3</sub> (up to x=0.15) is similar to that of pure CaRuO<sub>3</sub>(Ru<sup>4+</sup>, 4d<sup>4</sup>:t<sub>2g</sub><sup>4</sup>e<sub>g</sub><sup>0</sup> with S=1), however the Fe induces a ferromagnetic structure. Felner and Asaf [2] have reported recently about the magnetic properties of (Ca,Sr)RuO<sub>3</sub>. The mixed ruthenates with higher Sr contents show ferromagnetic behavior, the increase of saturation moment, and the decrease of coercive field.

In order to confirm the above phenomena, Ca<sub>1-x</sub>Sr<sub>x</sub>RuO<sub>3</sub> doped with 1% and 2% <sup>57</sup>Fe were prepared by a sol-gel method, and were

measured by Mössbauer spectroscopy at low temperatures. Sr rich ruthenates are tetragonal, and Ba ruthenates are cubic structures. Only Sr ruthenates doped with 1%<sup>57</sup>Fe and 2%<sup>57</sup>Fe showed the same ferromagnetic properties under 165K. Paramagnetic peaks and sextet peaks were coexisting between 153K and 94K. From IS, the doped Fe species showed only 3+, and the equivalent Ru ions become 5+. Mössbauer spectra of Ca<sub>1-x</sub>Sr<sub>x</sub>RuO<sub>3</sub> doped with 2% Fe (x=0.8, 0.6) also showed magnetic splitting under 106K and 77 K..

## 2P06 : Influence of counter anions on the rate of electron transfer in mixed-valence complexes [Fe<sub>2</sub>(bpmp)(ppa)<sub>2</sub>]X<sub>2</sub>

Yamamoto, M., Hayami, S., Maeda, Y. (Kyushu Univ.)

Mixed-valence  $\mu$ -phenolate-bis( $\mu$ -carboxylate)-bridged diiron(II,III) complexes show dynamics of electron transfer which is affected by the coordination environment of the complex and by the nature of ligands directly coordinated to the metal ions. In present work, to investigate the influence of the counter anions on the electron transfer rate, [Fe<sub>2</sub>(bpmp)(ppa)<sub>2</sub>](BF<sub>4</sub>)<sub>2</sub> (**1**), [Fe<sub>2</sub>(bpmp)(ppa)<sub>2</sub>](ClO<sub>4</sub>)<sub>2</sub>·2H<sub>2</sub>O (**2**), [Fe<sub>2</sub>(bpmp)(ppa)<sub>2</sub>](PF<sub>6</sub>)<sub>2</sub>·2H<sub>2</sub>O (**3**), and [Fe<sub>2</sub>(bpmp)(ppa)<sub>2</sub>](BPh<sub>4</sub>)<sub>2</sub>·3H<sub>2</sub>O

(**4**) were prepared, where Hbpmp represents 2,6-bis[bis(2-pyridylmethyl)aminomethyl]-4-methylphenol and Hppa,  $\beta$ -phenylpropionic acid. The Mössbauer spectra were measured for the complexes, and the complex **1**, **2**, and **3** show valence trapped doublets assigned to Fe<sup>II</sup> and Fe<sup>III</sup> at all temperature measured. As the temperature is increased, the two doublets approach each other, but remain even at 295 K. On the other hand, the complex **4** shows valence detrapped Mössbauer spectra at both 80 K and 295 K. The observed isomer shift value at 295K, 0.66 mm s<sup>-1</sup> is in the mean value of those for high-spin Fe<sup>II</sup> and high-spin Fe<sup>III</sup>, which means that the inverse of the electron transfer rate is comparable to the Mössbauer timescale or shorter at both 80 K and 295 K.

## 2P07 : Mössbauer resonance absorption in FePS<sub>3</sub> single crystal

Muramatsu, H., Tanaka, S. (Shinshu Univ.)

We have already reported a large deficit in absorption on Mössbauer spectrum taken with a mineral siderite, FeCO<sub>3</sub>, which shows antiferromagnetic behavior below 38.3 K, when the states |J=3/2, m=-3/2> and |J=3/2, m=1/2> cross and are mixed at 30.5 K. The deficit in absorption was explained as an interference of the two transition amplitudes corresponding to the two lines that occur at the same energy. As to a large deficit of absorption without any external magnetic field, a possible explanation would be the existence of inhomogeneities or imperfection in FeCO<sub>3</sub> crystal inducing a mixing interaction. For the single crystal of FeCO<sub>3</sub> synthesized in a laboratory, however, it seems

so hard to make large single crystal enough to be used as an absorber. Then, we tried to seek another absorber possible to use in the same type of experiment. The only candidate we found so far was the single crystal of FePS<sub>3</sub>. From a series of Mössbauer measurements using FePS<sub>3</sub> absorber, it was concluded that the hyperfine field of FePS<sub>3</sub>, about 9T in a saturation value, is not enough to make the absorption lines of (-3/2, -1/2) and (1/2, -1/2) merge into one single line, in order to observe EIT.

## 2P08 : <sup>57</sup>Fe Mossbauer spectra for 2D coordination polymer Fe(pz)<sub>2</sub>Ni(CN)<sub>4</sub>

Kitazawa, T., Matsubara, T., Takahashi, M., Takeda, M. (Toho Univ.)

Two dimensional coordination polymer Fe(pz)<sub>2</sub>Ni(CN)<sub>4</sub> (pz = pyrazine) has been prepared and measured by <sup>57</sup>Fe Mossbauer spectroscopy. The Mossbauer parameters indicate that spin states of iron(II) are high spin state both at 290 K and 77 K. Although 3D coordination polymer [Fe(pz)Ni(CN)<sub>4</sub>] reported by Real group shows cooperative spin crossover behavior, the 2D coordination polymer Fe(pz)<sub>2</sub>Ni(CN)<sub>4</sub> does not.

## 2P09 : <sup>57</sup>Fe Mössbauer spectroscopy of Jarosites produced in different areas and decomposed thermally

Iiyama, T.<sup>a</sup> Sakai, H.<sup>b</sup> Nomura, K.<sup>c</sup> Takahashi, M.,<sup>a</sup> Takeda, M.<sup>a</sup> (<sup>a</sup>Fac. of Sci., Toho Univ., <sup>b</sup>Professor Emeritus of Okayama Univ., <sup>c</sup>Grad. School of Eng., Univ. of Tokyo)

NASA reported in March 2004 that Mars-Exploration-Rovers Opportunity found the iron sulfate mineral, Jarosites, MFe<sub>3</sub>(OH)<sub>6</sub>(SO<sub>4</sub>)<sub>2</sub> (M = K, Na, H<sub>3</sub>O) in Meridiani Planum on Mars in fairly large area via <sup>57</sup>Fe Mössbauer spectroscopy. This proves the existence of water in past on Mars. However any value of their Mössbauer parameters are not yet published. This motivated us to carry out Mössbauer spectroscopic study on Jarosites produced on the Earth in different areas and their products by heating. We found that there are two iron sites in each Jarosite and the Mössbauer parameters of products by heating are different from those of Fe<sub>2</sub>(SO<sub>4</sub>)<sub>3</sub> and Fe<sub>2</sub>O<sub>3</sub> small particles.

## 2P10 : Mössbauer study on Fe/S films produced by laser ablation of pyrite

Yokoyama, D.,<sup>a</sup> Namiki, K.,<sup>a</sup> Yamada, Y.<sup>a</sup> (<sup>a</sup>Tokyo University of Science)

In this study, we report Fe/S films on aluminum and silicon substrates produced by laser-evaporation of pyrites. Laser light from YAG-laser was focused by a convex lens onto a target crystal in a

vacuum vessel. Laser-evaporated atoms were deposited on a substrate (Al or Si). The temperature of the substrate was kept at desired temperature (10~600 K) using a closed-cycle helium refrigerator and a resistive heater. Mössbauer spectra of the samples at room temperature were measured in transmission geometry with  $^{57}\text{Co}/\text{Rh}$  source using Wiessel MDU1200. The Mössbauer spectrum of the film produced by laser-evaporation of  $\text{FeS}_2$  deposited on Al substrate at room temperature consists of two components: doublet and sextet absorptions. The doublet absorptions is assigned to  $\text{FeS}_2$  having the same composition with the target material, and sextet absorptions is assigned to FeS. Sulfur atoms are less trapped than iron atoms on the deposition process. Relative yields of FeS/  $\text{FeS}_2$  in a film varied depending on experimental conditions. We also observed the shape of the films using scanning electron microscopy (SEM).

## **2P11 : Mossbauer Study on Iron Films Produced by Laser Ablation**

Namiki, K.<sup>a</sup> Yokoyama, D.<sup>a</sup> Yamada, Y.<sup>a</sup> (<sup>a</sup>Tokyo University of Science)

In this study, we report iron film on aluminum and silicon surface produced by laser-evaporation. Laser light from YAG-laser(NewWave, TEMPEST 10, 532nm, 88.9mJ/pulse, 5ns ) was focused by a convex lens onto a block of enriched  $^{57}\text{Fe}$  metal in a vacuum vessel( $10^{-5}$ pa).Laser-evaporated iron atoms were deposited on a substrate(Al or Si). The temperature of the substrate was kept at desired temperature (10~600K) using a closed-cycle helium refrigerator (Iwatani CryoMini) and a resistive heater. The amount of iron, the thickness of the film, was controlled by the laser irradiation time. Mossbauer spectra of the samples at room temperature were measured in transmission geometry with  $^{57}\text{Co}/\text{Rh}$  source using Wiessel MDU1200. The iron films deposited on Si crystals were studied to see the influence of substrate materials. We also observed the shape of the films using scanning electron microscopy (SEM) (Hitachi S-5000) and compared with their Mossbauer spectra.

## **2P12 : $^{197}\text{Au}$ Mössbauer Spectra for polynuclear gold(I) complexes having 1,1'-Bis(diphenylphosphino)ferrocene as a bridging ligand**

Kang, Y., Takahashi, M., Takeda, M. (Toho Univ)

1,1'-Bis(diphenylphosphino)ferrocene(dppf) acts as a chelating-or bridging ligand. Although many dppf gold complexes such as  $(\text{dppf})_2\text{Au}^{\text{I}}$  and  $(\text{dppf})_2\text{Au}^{\text{III}}$  have been known , only a few are reported for multinuclear gold(I) dppf complexes. This work is carried out to the electronic states of dppf gold(I) complexes and to examine the multinuclization of  $[(\text{dppf})\text{Au}^{\text{I}}]^{\text{2+}}$  unit.

The reaction of dinuclear gold complex  $\text{dppf}(\text{AuCl})_2$  with ligands ( $\text{Na}_2\text{S}$ ,  $\text{KSCN}$ ,  $\text{HSC}_6\text{H}_4\text{CH}_3$ ,  $\text{Ag}(\text{tht})\text{ClO}_4$ ,  $\text{HSC}_6\text{H}_4\text{COOH}$  and  $\text{NaSH}$ ) gave  $[(\text{dppf})\text{Au}]_2(\text{dt})$ ,  $(\text{dppf})\text{Au}_2\text{S}$  (A),  $(\text{dppf})[\text{AuSCN}]_2$  (B),  $(\text{dppf})[\text{AuSC}_6\text{H}_4\text{CH}_3]_2$  (C),  $[(\text{dppf})\{\text{Au}(\text{tht})\}_2](\text{ClO}_4)_2$ ,  $(\text{dppf})[\text{AuSC}_6\text{H}_4\text{COOH}]_2$  and  $(\text{dppf})[\text{AuSH}]_2$ . The reaction of  $(\text{dppf})[\text{AuCl}]_2$  with B gave tetranuclear gold complex  $[(\text{dppf})(\text{AuSCNAu})_2(\text{dppf})](\text{OTf})_2$ .

$^{197}\text{Au}$  Mössbauer spectra were measured for A, B and C at 12K. These have relatively large isomer shifts( $\delta$ ) and quadrupole splitting( $\Delta$ ) since these have the soft donor such as P and S. Interestingly  $\delta$  and  $\Delta$  for C were larger than those of  $[\text{Au}^{\text{I}}(\text{SR}_2)(\text{PPh}_3)]^+$  (R=Me, Ph) having the same donor atoms.

## **2P13 : Preparation and electronic state of dinuclear cycroaurated complexes with arsine-containing ligand**

Kitadai, K.<sup>a</sup>, Takahashi, M.<sup>a</sup>, Takeda, M.<sup>a</sup>, Bhargava, S.K.<sup>b</sup>, Prever,S.<sup>b</sup>, Bennett, M.A.<sup>c</sup>(Toho Univ.<sup>a</sup>, RMIT Univ.<sup>b</sup>, Australian National Univ.<sup>c</sup>)

Cyclometalated gold compounds containing arsenic atom are investigated by x-ray crystallography and  $^{197}\text{Au}$  Mössbauer spectroscopy. The dinuclear gold(I) complex  $[\text{Au-C}_6\text{H}_3(\text{Me})\text{AsPh}_2]_2$  reacts with halogens ( $\text{PhiCl}_2$ ,  $\text{Br}_2$ ,  $\text{I}_2$ ) at low temperatures to form the dinuclear gold(II) complexes  $[\text{X-Au-C}_6\text{H}_3(\text{Me})\text{AsPh}_2]_2$ , in which Au-Au distances are decreased in the order of  $\text{X = I} > \text{Br} > \text{Cl}$  by about 10 pm.  $^{197}\text{Au}$  Mössbauer isomer shifts and quadrupole splittings for dinuclear gold(I) complexes are smaller than those of corresponding phosphine complex, suggesting the weaker Au-As interactions.

## **2P14 : Study of $\text{V}_2\text{O}_5\text{-B}_2\text{O}_3\text{-Li}_2\text{O}$ glasses containing $\text{Fe}_2\text{O}_3$ (10mol%)**

Watanabe, C., katada, M (Graduate School of Science,Tokyo Metropolitan Univ.)

In this study, we prepared three-component system glasses of  $\text{V}_2\text{O}_5\text{-B}_2\text{O}_3\text{-Li}_2\text{O}$ . In the first, we determined the glass-forming region by XRD. In the next, we investigated the local structure of  $\text{V}_2\text{O}_5\text{-B}_2\text{O}_3\text{-Li}_2\text{O}$  glasses by Mössbauer and IR studies to elucidate a short-range order structure of those glasses. The glass-forming region of  $\text{V}_2\text{O}_5\text{-B}_2\text{O}_3\text{-Li}_2\text{O}$  series was found in high  $\text{Li}_2\text{O}$  containing area. The glass-forming region was expanded to lower  $\text{Li}_2\text{O}$  containing area by adding  $\text{Fe}_2\text{O}_3$  (10mol%) to the glasses. The values of isomer shifts (IS) and quadrupole splitting (QS) for the glasses were  $0.35\sim0.42\text{mmms}^{-1}$  and  $0.65\sim1.09\text{mmms}^{-1}$  respectively. These parameters were affected by not only  $\text{Li}_2\text{O}$  ratio but also  $\text{V}_2\text{O}_5$  and  $\text{B}_2\text{O}_3$  ratio.

## **2P15 : Introduction of organic compounds to assembled complexes and their Mössbauer spectroscopic study**

Morita, T.<sup>a</sup> Nakashima, S.,<sup>b</sup> Okuda, T.<sup>a</sup> (<sup>a</sup>Fac. of Sci., Hiroshima Univ.,  
<sup>b</sup>N-BARD, Hiroshima Univ.)

The inclusion of organic compound (biphenyl) similar to the ligand molecule was confirmed using X-ray structural analysis and the electronic change was investigated by <sup>57</sup>Fe Mössbauer spectroscopy. The composition was confirmed by the X-ray structural analyses as Fe<sub>2</sub>(NCS)<sub>4</sub>(bpy)<sub>4</sub>(biphenyl)<sub>5</sub>, Fe(NCS)<sub>2</sub>(bpa)<sub>2</sub>(biphenyl)<sub>2</sub>, and Fe(NCSe)<sub>2</sub>(bpa)<sub>2</sub>biphenyl. <sup>57</sup>Fe Mössbauer spectroscopy revealed that the QS values changed depending on the structure and the electric field gradient reverses depending on the structure of the bpa complex.

#### 2P16 : A neutron in-beam Mössbauer spectrum of iron disulfide

Kubo, M. K.,<sup>a</sup> Kobayashi, Y.,<sup>b</sup> Nemoto, Y.,<sup>c</sup> Yamada, Y.,<sup>c</sup> Sakai, Y.,<sup>d</sup> Shoji, H.,<sup>c</sup> Yonezawa, C.,<sup>f</sup> Matsue, H.<sup>f</sup> (<sup>a</sup>Intern. Christ. Univ.,<sup>b</sup>RIKEN,  
<sup>c</sup>Tokyo Univ. Sci.,<sup>d</sup>Daido Inst. Tech.,<sup>e</sup>Tokyo Metro. Univ.,<sup>f</sup>JAERI)

A room temperature neutron in-beam <sup>57</sup>Fe Mössbauer spectrum of iron disulfide was measured at the PGA port of JRR-3M in JAERI with a parallel plate avalanche counter. While the absorption spectrum of the target material shows one doublet line with a small quadrupole splitting arising from the low spin ferrous configuration, the emission spectrum obtained in this work was consisted of two doublets having different QS values with a 2 to 1 intensity ratio. The component with a large QS, clearly different from the parent compound, evidenced that there occurred some chemical change after the (n, gamma) reaction. Both components were tentatively assumed to be Fe(0) species due to the IS values of nearly 0 mm s<sup>-1</sup>.

#### 2P17 : <sup>151</sup>Eu Mössbauer spectroscopic and powder X-ray diffraction method study on local structure around Eu ions in a variety of fluorite-type structure oxides

Masaki, N.,<sup>a</sup> Otoba, H.,<sup>a</sup> Nakamura, A.,<sup>a</sup> Doi, Y.,<sup>b</sup> Hinatsu, Y.<sup>b</sup>  
(<sup>a</sup>JAERI, <sup>b</sup>Hokkaido Univ.)

Fluorite-type oxides, MO<sub>2</sub> (M=Zr, Hf, Ce, U, Th, etc.), containing Eu<sup>3+</sup> ion were synthesized by using conventional ceramics method. X-ray diffraction pattern of the samples was analyzed by Rietveld method in order to get long-range structure of the oxides, phase, lattice constant etc. From the behavior of isomer shifts (IS) and quadrupole splittings obtained with Mössbauer spectra, we can get the information of local structure around Eu<sup>3+</sup> ions by comparing with the long-range structure. For M=Hf, Zr systems, oxide solid solution Eu<sub>x</sub>M<sub>1-x</sub>O<sub>2-x/2</sub> (x=0.5) has pyrochlore phase in which both cation and anion are ordered. The value of IS is about 0.5 mm/s and it means that the coordination number (CN) of oxygen ion around Eu<sup>3+</sup> is eight. For M=U (0<x<0.5),

U<sup>4+</sup> ion is oxidized to U<sup>5+</sup> by substitution of U<sup>4+</sup> with Eu<sup>3+</sup> and the IS values are about 0.5 mm/s, which shows the CN is 8.

#### 2P18 : <sup>237</sup>Np Mössbauer Spectra and Correlation for Neptunyl(VI) Complex Coordinated 2,2'-bipyridyl

Kawasaki T.,<sup>1</sup> Kitazawa T.,<sup>1</sup> Takeda M.,<sup>1</sup> Nakada M.,<sup>2</sup> Sacki M.<sup>2</sup> (<sup>1</sup>Fac. Sci. Toho Univ., <sup>2</sup>Jpn. At. En. Res. Inst.)

The complex was synthesized from acetonitrile solution of neptunyl(VI) nitrate by adding acetonitrile solution of 2,2'-bipyridyl in glove box at room temperature. The characterization was made by XRD. <sup>237</sup>Np Mössbauer spectra were measured at 11, 30, 50 K. The absorption lines due to quadrupole and magnetic splitting were observed.

#### 2P19 : Photo-controllable magnetic iron oxide nano-particles

Einaga, Y., Mikami, R., Taguchi, M., Yamada, K., Suzuki, K., Sato, O.  
(Keio Univ., KAST)

We present a novel method for the preparation of reversibly photo-controllable magnetic nanoparticles that even works at room temperature.  $\gamma$ -Fe<sub>2</sub>O<sub>3</sub> magnetic nanoparticles, with an estimated average size of 5 nm, were encapsulated with n-octylamine and an azobenzene-containing amphiphilic compound. Photoisomerization of the azo moiety affected the electrostatic field around the  $\gamma$ -Fe<sub>2</sub>O<sub>3</sub> magnetic nanoparticles. As a result, we were able to reversibly control the magnetic properties of this composite material by photo-illumination in the solid state at room temperature.

#### 2P20 : Mössbauer and XAFS spectroscopic studies of (Y,Zr)-Np-O systems

Nakada, M.,<sup>a</sup> Otobe, H.,<sup>a</sup> Yamashita, T.,<sup>a</sup> Akabori, M.,<sup>a</sup> Minato, K.,<sup>a</sup> Motohashi, H.<sup>b</sup> (<sup>a</sup>JAERI, <sup>b</sup>TNS)

Cubic stabilized zirconia and zirconium pyrochlores are useful for nuclear and non-nuclear fields. Yttria stabilized zirconia is the popular and promising material because of its wide range of stability in the phase diagram. The single phase of Np-doped yttria stabilized zirconia were confirmed by powder X-ray diffraction techniques. Lattice parameters of (Y,Zr)<sub>0.95</sub>Np<sub>0.05</sub>O<sub>2-x</sub> and (Y,Zr)<sub>0.8</sub>Np<sub>0.2</sub>O<sub>2-x</sub> were about 0.5155 and 0.5209 nm, respectively. <sup>237</sup>Np Mössbauer spectra were measured transmission geometry at low temperatures. Np(IV) and small amount of Np(V) species were observed in (Y,Zr)<sub>0.8</sub>Np<sub>0.2</sub>O<sub>2-x</sub> by the Mössbauer spectroscopy. XANES spectra of Y, Zr and Np elements in (Y,Zr)<sub>0.95</sub>Np<sub>0.05</sub>O<sub>2-x</sub> showed almost the same chemical states for that in (Y,Zr)<sub>0.8</sub>Np<sub>0.2</sub>O<sub>2-x</sub>.

## **2P21 : Radionuclides released from pneumatic tubes in research reactor facilities**

Oki, Y.<sup>a</sup> Ozaki, A.,<sup>b</sup> Kaneto, T.,<sup>b</sup> Hata, Y.,<sup>c</sup> Takamiya, K.,<sup>a</sup> Shibata, S.,<sup>a</sup> Yamasaki, K.<sup>a</sup> (<sup>a</sup>Res. Reactor Inst., Kyoto Univ., <sup>b</sup>Grad. School of Eng., Kyoto Univ., <sup>c</sup>Dept. of Eng., Kyoto Univ.)

Radionuclides are released from pneumatic tubes into hot cells when irradiation capsules are transported from the reactor core to hot cells by the pneumatic transport system in research reactors. We collected both of radioactive aerosols and radioactive gases released from the tube in the Kyoto University Reactor, and analyzed their radioactivities. Aerosol size was also analyzed with a low pressure impactor. Many kinds of FP nuclides were observed in both of the aerosols and the gases. In addition, non-FP nuclides (<sup>24</sup>Na, <sup>56</sup>Mn) were also detected only in the aerosol samples. The pneumatic tube at the reactor core is made of aluminum. FP nuclides were considered to be emitted into the tube by recoil from uranium contained as impurity in the aluminum tube, while non-FP nuclides are formed by activation of airborne dusts in the tube. Particle diameter for FP nuclide aerosols was found to be 0.3–0.8 μm, which was always smaller than that for non-FP nuclides (ca. 1μm).

## **2P22 : Size distribution of radioactivity in aerosol**

Fukuda, A.<sup>1</sup>, Momoshima, N.<sup>2</sup> (<sup>1</sup>Grad. Sch. Sci. Tec., Kumamoto Univ., <sup>2</sup>Fac. Sci., Kumamoto Univ.)

Size of aerosols was a major factor that controls the behavior of aerosols in the atmosphere. The objective of this study was to determine the aerodynamic size distributions and the activity median aerodynamic diameters (AMAD) of natural radioactive nuclides existing in the atmosphere. Aerosols were separated into 13 stages with a low-pressure cascade impactor, collecting at Kumamoto University (35.7 m above the ground). <sup>7</sup>Be (half-life: 53.3 d), <sup>210</sup>Pb (half-life: 22.3 y), <sup>210</sup>Po (half-life: 138 d), and <sup>212</sup>Pb (half-life: 10.6 h) were determined by γ- or α-spectrometry, and the AMAD of each nuclide was obtained. SO<sub>4</sub><sup>2-</sup> was determined by ion chromatograph. The distribution of <sup>7</sup>Be, <sup>210</sup>Pb and <sup>210</sup>Po was largely associated with aerosols around 1.0 μm. The distribution of SO<sub>4</sub><sup>2-</sup> was similar to that of <sup>7</sup>Be, <sup>210</sup>Pb and <sup>210</sup>Po. The <sup>212</sup>Pb showed a distribution extended to smaller in size. The AMADs of <sup>212</sup>Pb, <sup>7</sup>Be, <sup>210</sup>Po and <sup>210</sup>Pb were 0.37 μm, 0.52 μm, 0.78 μm and 0.69 μm, respectively, indicating a tendency that the nuclide with a longer half-life has the larger AMAD.

## **2P23 : <sup>137</sup>Cs in recent fallout samples in relation to the Asian Continent aerosols (3)**

Ishikawa, Y., Takahashi, M. (Environ. Radioact. Res. Inst. Miyagi),

Narazaki, Y. (Fukuoka Inst. Health & Environ. Sci.), Suzuki, T. (Fac. of Sci., Yamagata Univ.)

<sup>137</sup>Cs deposition (rain and dry fallout) was investigated from July 2002 in Miyagi and Yamagata Prefs., Japan. Higher values of <sup>137</sup>Cs deposition were observed in Sakata City, faced to the Japan Sea, than in other inland provinces (Yamagata City and Sendai City) or in the eastern area (Onagawa Town, faced to the Pacific). The sample collected during Mar. 9-Apr. 13, 2004, when the Japan Meteorological Agency has observed the Asian Continental Dust Event (Kosa) in Sakata City, showed the highest value of <sup>137</sup>Cs (about 120 mBq m<sup>-3</sup> / 30 d ). This fact probably shows the contribution of the aerosol-derived <sup>137</sup>Cs due to the Asian Continent.

## **2P24 : Atmospheric concentration of <sup>210</sup>Pb, <sup>212</sup>Pb and <sup>7</sup>Be at Tsukuba**

Doi, T.<sup>a</sup> Sato, J.<sup>b</sup> (<sup>a</sup>Natl. Inst. Environ. Stud., <sup>b</sup>School of Sci. and Tehnol., Meiji Univ.)

Continuous measurement of atmospheric concentrations of <sup>210</sup>Pb, <sup>212</sup>Pb and <sup>7</sup>Be were carried out from 1987 to 1999 at Tsukuba, Japan. Monthly averaged atmospheric concentrations of <sup>7</sup>Be, <sup>210</sup>Pb and <sup>212</sup>Pb ranged 1 - 7 mBq/m<sup>3</sup>, 0.2 - 0.8 mBq/m<sup>3</sup> and 10 - 160 mBq/m<sup>3</sup>, respectively. The atmospheric <sup>7</sup>Be and <sup>210</sup>Pb concentrations showed “two-peak” variation pattern : high concentrations were recorded in spring and fall. Atmospheric <sup>212</sup>Pb concentration showed “one-peak” variation pattern : the maximum levels were appeared in winter. Seasonal variation of <sup>210</sup>Pb concentration was interpreted that a part of <sup>222</sup>Rn emitted from the ground surface may be transported to the upper part of the atmosphere and long-lived <sup>210</sup>Pb accumulated in the lower part of the stratosphere behaved similarly to the cosmogenic <sup>7</sup>Be produced in the stratosphere, and they subsided into the troposphere through the tropopause break during spring, and also by the migratory anticyclones passing frequently over Japan during spring and fall. Seasonal variations of <sup>212</sup>Pb concentration may be dependent on the seasonal variation of the duration of the nocturnal inversion layer.

## **2P25 : Depth Profiles of Environmental Neutron Flux in Water**

Hamajima, Y., and Komura, K. (LLRL, Kanazawa University)

Depth profiles of environmental thermal neutron flux in water were measured using activation technique. It was difficult to measure the profile in water up to the present, because of extremely low intensity of the flux. Radioactivity in gold target was measured at once by the ultra-low-level measurement system of Ge detectors in Ogoya Underground Laboratory, where 5 well, 4 planer, and 1 coaxial type Ge

detectors with high efficiency were set up. A significant difference was not seen in the depth profiles between the fresh water and the seawater. The environmental thermal neutron flux in water was decreased exponentially as a function of depth. There seems to be a small gap in 20 to 30 g/cm<sup>2</sup>. In some cases, a peak was found at around 5 g/cm<sup>2</sup>. These results were almost consistent with the calculation results of Kastner et al. (1970). According to the result of the calculation, the neutron flux varies rapidly with the boundary of atmosphere and hydrosphere. The peak of shallow depth might be this effect.

## 2P26 : Transport calculation of neutrons leaked in the environment by the JCO criticality accident

Imanaka, T. (Res. Reactor Inst., Kyoto Univ.)

Neutron behavior in the environment at the time of the JCO criticality accident was simulated using 3-dimensional Monte Carlo transport codes, MORSE-CG and MCNP/4C. Neutron leakage spectrum from the precipitation tank in which 18.8 %-enriched uranyl nitrate solution became supercritical was obtained based on criticality calculation in the tank. Using this leakage spectrum, 3-dimensional neutron transport calculations in the environment were performed up to 600 m from the source point, taking into consideration various shielding structures. Our calculation could reconstruct neutron doses measured along the JCO site boundary within 50 % errors. Concerning calculations for neutron induced radionuclides, thermal neutron reactions were reconstructed satisfactorily, while calculated values for fast neutron reactions were larger than measurements. In order to clarify the discrepancy for fast neutron reactions, detailed calculations are now underway for shielding effects of houses and adjacent structures.

## 2P27 : Uranium and thorium isotopes in lake bottom sediment -Lake Baikal-

Sakaguchi, A.,<sup>a</sup> Yamamoto, M.,<sup>a</sup> Tomita, J.,<sup>a</sup> Kashiwaya, <sup>b</sup>K., Kawai, T.<sup>c</sup>  
(<sup>a</sup> LLRL Kanazawa Univ. <sup>b</sup> Graduated School of Natural Sci. and Technol., Kanazawa Univ. <sup>c</sup> Faculty of Sci. Nagoya Univ.)

Studies on sedimentary behavior of U (Th) have been performed using about 60 cm depth sediment core of Lake Baikal in the light of the linkage to paleoenvironmental changes as follows: depth profiles of U and Th isotopes, distribution of lithogeneous and autogenous U in the sediment, geochemical association of them with sediment components by sequential leaching method and relationship between U content and some parameters such as grain size, biogenic-SiO<sub>2</sub>, etc.

These isotopic concentrations and their ratios varied widely with depth of sediment core. A marked radioactive disequilibrium (1.53 - 1.81) higher than the value of 1.0 was observed for <sup>234</sup>U/<sup>238</sup>U activity ratios, indicating that U from lake water with high <sup>234</sup>U/<sup>238</sup>U ratio (ca.

2.0) was transferred to the bottom sediment by adsorption and/or adhesion onto the settling particles. The results obtained here suggest that variation in the lithogenous and/or autogenous U in the sediment with depth might be helpful in tracing the behavior of U.

## 2P28 : Anomalously high U accumulation in some pond and lake sediments from areas surrounding the Semipalatinsk nuclear test site

Yamamoto, M.,<sup>a</sup> Sakaguchi, A.,<sup>a</sup> Hoshi, M.,<sup>b</sup> Takada, J.,<sup>c</sup> B. I. Gusev,<sup>d</sup>  
(<sup>a</sup>LLRL Kanazawa Univ, <sup>b</sup> Hiroshima Univ., <sup>c</sup>Sapporo Medical Univ.,<sup>d</sup>Research Inst. Medical and Ecology, Kazakhstan Republic.)

Sediment core samples up to a depth of 25-40 cm were collected from three ponds (P. Korosteli, P. Mihairov and P. Alkat) and two lakes (L. Kanoneruka and L. Semanaika) located in widely separated regions outside the former Semipalatinsk nuclear test site (SNTS) in Kazakhstan. The U, including <sup>137</sup>Cs and Pu, were determined in samples subdivided at 1cm intervals from the top of each core. These sediment cores were dated by excess <sup>210</sup>Pb method. The reservoirs with low sedimentation rates of 0.038- 0.41 g/cm<sup>2</sup>/y permitted, not in details, estimating the temporal history of close-in fallout of <sup>137</sup>Cs and Pu from the SNTS in the areas studied. The sediments accumulating an anomalously high <sup>238</sup>U of 250-400 Bq/kg were also found for two among five reservoirs, in which their <sup>234</sup>U/<sup>238</sup>U and <sup>235</sup>U/<sup>238</sup>U activity ratios are 1.3-2.0 and around 0.047 (nearly the same as that of natural U), respectively. Such U enrichment at subsurface with a thin layer of lower-U sediment at surface is mainly due to infiltration of lake water containing U from the ground waters flowing into the lake or pond, followed by reduction of U(VI) to U (IV) at the redox boundary.

## 2P29 : Detection of Co-60 in the liver of octopus caught in the East China Sea

Morita, T., Fujimoto, K., Nishiuchi, K., Kimoto, K., Minakawa, M., Yoshida, K. (Fisheries Research Agency)

Fisheries Research Agency carries out a long term monitoring program for radioactive pollution in marine organisms caught around Japan in order to confirm the safety of these organisms as a food source. Recently, Co-60 (physical half-life = 5.7 years) has been detected in the livers of octopus, *Octopus vulgaris*, caught in the East China Sea. The concentration of Co-60 tends to decrease gradually. In order to specify the pollution source of the Co-60, we analyzed the livers of octopus from the various sea areas. Our results indicated that the nuclear pollution source was not along the Japanese coast. However, the nuclear pollution source has been unclear yet.

## 2P30 : Studies on distribution of radionuclides around

## Kashiwazaki-Kariwa area

Sakaue, H.<sup>1</sup>, Maruta, F.<sup>1</sup>, Fujimaki, H.<sup>1</sup>, Tonouchi, S.<sup>1</sup> and Hashimoto, T.<sup>2</sup> (Niigata Prefectural Institute of Environmental Radiation Monitoring<sup>1</sup>, Faculty of Science, Niigata Univ.<sup>2</sup>)

Radioactivity surveys of some environmental samples such as rain and dry fallout, fresh water, soil and lake sediments were conducted at Kashiwazaki-Kariwa area for estimation of background level. Gamma ray spectrometry by Ge semiconductor detector was used for all samples after drying and/or evaporation of water. One of most characteristic radionuclides was <sup>137</sup>Cs which reflects local information of each sampling point. Greater emphasis was placed on some fresh water samples from rivers around Mt. Yoneyama which showed <sup>137</sup>Cs in slightly higher content. The results were discussed concerning with topographical and geological features of Mt. Yoneyama, where a place of rich in fallout radionuclides may be identified.

## 2P31 : <sup>228</sup>Ra/<sup>226</sup>Ra ratio of coastal water in the Noto Peninsula

Watanabe.S., Inoue.M., Kofuji.H., Yamamoto.M. and Komura.K. (LLRL, Kanazawa Univ.)

In order to examine circulation of coastal water, 20L coastal water samples were collected from 7 sites of coastal areas in the Noto Peninsula, Japan. Radium isotopes in water samples were collected by coprecipitation with Ba<sup>2+</sup> carrier and measured by ultra low background  $\gamma$ -ray spectrometry.

The <sup>228</sup>Ra/<sup>226</sup>Ra activity ratio of these water samples exhibited seasonal variation with minimum values in August and maximum values in December, which was mainly dominated by changes in <sup>228</sup>Ra activity around these coastal areas.

## 2P32 : Tritium level in the Rokkasho-mura, Japan surrounding areas of the nuclear fuel reprocessing plant during the pre-operational period

Kakiuchi, H., <sup>a</sup>Iyogi, <sup>a</sup>T., Shino, M., <sup>b</sup>Hisamatsu, S., <sup>a</sup>Inaba, J. (<sup>a</sup>IES, <sup>b</sup>Tohoku Nuclear)

To assess the concentration level of tritium in Rokkasho-mura in Aomori Prefecture, Japan before the nuclear fuel reprocess plant operated, tritium concentration were measured in precipitation, inland waters, FWT (free water tritium), and OBT (organically bound tritium). The tritium concentration at Rokkasho-mura almost was attenuated to the stationary state, and tritium concentration in FWT and OBT were almost the same levels as that in precipitation.

## 2P33 : Distributions and downward velocities of <sup>239+240</sup>Pu,

## <sup>137</sup>Ca and <sup>210</sup>Pb in un-disturbed fields in Rokkasho, Japan

Ohtsuka, Y., Iyogi, T., Kakiuchi, H., Hisamatsu, S., Inaba, J. (Inst. Environ. Sci.)

Japan's first commercial nuclear fuel reprocessing plant is now being constructed in Rokkasho Village, Japan, and will be completed in 2007. Since a large amount of plutonium and fission products will be handled in the plant, it is important of investigate background levels of Pu and other related radionuclides in soil around the plant. In this study, distributions and downward velocities of <sup>239+240</sup>Pu, <sup>137</sup>Ca and <sup>210</sup>Pb in un-disturbed fields in the village were examined. About 90% of each nuclide exists in upper layer soils than 13 cm deep. Inventories of <sup>239+240</sup>Pu, <sup>137</sup>Ca and excess <sup>210</sup>Pb in un-disturbed fields in Rokkasho were  $81 \pm 21$  Bq m<sup>-2</sup>,  $2.3 \pm 0.8$  kBq m<sup>-2</sup> and  $14.5 \pm 1.7$  kBq m<sup>-2</sup>, respectively. Velocities of three nuclides in each depth were estimated from their fallout patterns and vertical distributions. Their velocities range 0.1-0.9 cm y<sup>-1</sup>, 0.3-0.7 cm y<sup>-1</sup> and 0.1-0.6 cm y<sup>-1</sup> for <sup>239+240</sup>Pu, <sup>137</sup>Ca and <sup>210</sup>Pb, respectively. There was good correlation between the velocity of <sup>239+240</sup>Pu and that of <sup>137</sup>Ca. The velocity of <sup>239+240</sup>Pu was 88% of <sup>137</sup>Ca, and showed the similar behavior of the both nuclides in soil environment.

## 2P34 : Distribution of atomic-bomb plutonium in surface soil at Nagasaki

Kokubu, S. Y.<sup>a</sup>, Magara, M.<sup>a</sup>, Miyamoto, Y.<sup>a</sup>, Sakurai, S.<sup>a</sup>, Usuda, S.<sup>a</sup>, Yamazaki, H.<sup>b</sup>, Yoshikawa, S.<sup>c</sup> (<sup>a</sup>JAERI, <sup>b</sup>Kinki Univ., <sup>c</sup>Osaka City Univ.)

The explosion of a plutonium atomic bomb over Nagasaki city took place on August 9, 1945. A large amount of fission products and unfissioned plutonium were released. The distribution of unfissioned plutonium within 8 km area from the hypocenter was determined by <sup>239+240</sup>Pu and <sup>240</sup>Pu/<sup>239</sup>Pu in soils. The prepared dry soil samples were treated with 8MHNO<sub>3</sub> after the addition of a known amount of <sup>242</sup>Pu as a spike. After separation of Pu with anion exchange resin, <sup>239</sup>Pu, <sup>240</sup>Pu and <sup>242</sup>Pu were determined by a double focusing ICP-MS. The <sup>239+240</sup>Pu concentrations in the soils collected at the east side of the hypocenter were higher than those in the west side. The <sup>240</sup>Pu/<sup>239</sup>Pu ratios in the soils at north, west and south side were similar to global fallout level. On the other hand, low <sup>240</sup>Pu/<sup>239</sup>Pu ratios in the soils at east of the hypocenter were found. The unfissioned Pu of the atomic bomb origin was deposited mainly around Nishiyama reservoir.

## 2P35 : A study on the distribution of iodine between soil and water based on the speciation of iodine both in soil and water

Kodama, S., Takahashi, Y. (Dep. of Earth and Planetary Systems Sci., Graduate School of Sci., Hiroshima Univ.)

The distribution of iodine between soil and water has been studied based on the speciation of iodine in water by HPLC-ICP-MS and in soil by X-ray absorption near-edge structure (XANES). For the speciation in soil, it was revealed that XANES at I K-edge is better for the I speciation in soil including water than I L-edge XANES. It was clearly shown based on the direct speciation in the two phases that the iodine distribution (soil/water) is much larger for  $\text{IO}_3^-$  than for  $\text{I}^-$ . The concentration of dissolved iodine increased under the reduced condition due to the formation of  $\text{I}^-$  species when  $\text{IO}_3^-$  was added to soil in our laboratory experiments. The speciation of iodine in natural soil samples showed that the present results are consistent with that by sequential extraction, though it was suggested that the direct speciation including three components ( $\text{I}^-$ ,  $\text{IO}_3^-$ , and organic iodine species) can be difficult in the deconvolution of the XANES spectra.

### **2P36 : Application of imaging plate to the measurement of natural uranium of extremely low-level activity**

Yasuda, K., Gunji, H., Sakurai, S., Usuda, S. (R&D Group for Environmental Technology, JAERI)

In order to effectively analyze the safeguards environmental swipe samples, information of nuclear material distribution on the swipe samples obtained by non-destructive analysis is very important. In this study, it was successfully demonstrated that the distributions of natural uranium from  $10^4\text{Bq}$  to the  $10^0\text{Bq}$  levels were measured by means of the imaging plate technique under a low background radiation condition. At presentation, technical problems for measuring extremely low-level radioactive materials by using the imaging plate technique will be reported.

### **2P37 : Radioactivity content of papers (III)**

Kobashi, A. (School of Science, Univ. of Tokyo)

The radioactivities of natural occurring radionuclides ( $^{226}\text{Ra}$ ,  $^{228}\text{Ra}$ ,  $^{228}\text{Th}$ , and  $^{40}\text{K}$ ) and a fallout nuclide ( $^{137}\text{Cs}$ ) in papers such as magazines and newspapers were determined by gamma-ray spectrometry to obtain information on radioactivity level of papers. The X-ray diffraction patterns of the samples were also measured to elucidate the sources of radionuclides contained in the papers. The average  $^{226}\text{Ra}$ ,  $^{228}\text{Ra}$ ,  $^{228}\text{Th}$ , and  $^{40}\text{K}$  contents of pocket-sized books were 6.4, 21.5, 23.7, and 18.8  $\text{Bq/kg}$ , respectively, and those of other kinds of samples were near to or less than the values. The concentrations of the natural occurring radionuclides were correlated to each other. Cesium-137 was detected in magazines and newspapers that contained mechanical pulp as a main

constituent. The X-ray diffraction study showed that kaolinite, talc, and calcite were contained in the papers. The kaolinite content of the samples was correlated to the concentrations of the natural occurring radionuclides, showing that the radioactivity in the paper samples was mainly brought with kaolinite used as filler or pigment in the papers.

### **2P38 : Determination of uranium and thorium in iron ore and iron and steel**

Takano,M.<sup>a</sup> Okada,Y.<sup>a</sup> Hirai,S.<sup>a</sup> Mitsugashira,T.<sup>b</sup> Hara,M.<sup>b</sup> (<sup>a</sup>Fac. of Eng., Musashi Inst. of Tech., <sup>b</sup>Inst. for Material Res., Tohoku Univ)

Uranium and thorium nuclides in JSS red iron ore, iron and stainless steel reference material, JSS 805-1 and JSS 803-4, were determined by applying the coprecipitation method with  $\text{SmF}_3$  (Sm method). The analytical samples were decomposed by a nitrohydrochloric acid or mixed acid solution of hydrochloric acid and hydrofluoric acid. Uranium and thorium of known activity were added to solution in the case of analysis of iron and stainless steel. Uranium and thorium were coprecipitated with neodymium fluoride to remove matrix iron. Then, uranium and thorium were purified and isolated separately by an anion-exchange chromatography. The uranium and thorium were finally collected in  $\text{SmF}_3$  precipitates and the precipitates were mounted as alpha-spectrometric samples. The chemical recovery yield was determined. The results of alpha-spectrometry were compared with added activity or the results of INAA and we confirmed that the chemical recovery yield was quantitative without separation of thorium in stainless steel.

### **2P39 : Fundamental studies of optically stimulated luminescence phenomena using natural quartz**

Yawata, T. (Doctoral Program in Natural Science, Niigata University), Hashimoto, T. (Department of Chemistry, Niigata University)

Some radiation-induced luminescence phenomena, such as thermoluminescence (TL), optically stimulated luminescence (OSL) from crystalline minerals, have been observed when some dielectric minerals were heated or stimulated after the irradiation. These luminescence phenomena from radiation-induced luminescent materials have been preferably utilized as personal dosimeters as well as for naturally accumulated dose-evaluations. In this study, some OSL-emission mechanical-properties from natural quartz grains were investigated using a new automated OSL/TL measuring system. This system includes sixteen blue LEDs (Nichia Co., Ltd) having a peak at 470 nm in the emission spectrum as a stimulation light for OSL measurements around violet region. Concerning the stimulation powers, OSL intensities tended to be saturated beyond  $10 \text{ mW/cm}^2$ . As a result, OSL phenomena were found to be greatly dependent on the measuring

conditions, such as applied LED powers, grain sizes, measuring temperatures and optical properties on the quartz-grain surface.

#### **2P40 : Dependence of TL-sensitivity changes from feldspar on different thermal annealing treatments**

Mitamura, N.<sup>a</sup>, Hashimoto, T.<sup>b</sup> (<sup>a</sup>Graduate School of Science and Technology, Niigata University., <sup>b</sup>Faculty of Science, Niigata University)

Feldspar has been expected for the use of luminescence dating because the luminescence sensitivity of feldspar generally shows much higher than that of quartz. The feldspar typically has two main emission bands. Since a blue emission (430 nm) is known to cause anomalous fading, the blue emission-range is not suitable to the dating application. Another range is a far-red emission around 730 nm that has been ascertained to be stable. Actually, the authors could confirm no-fading effect of far-red TL in seven-month stored feldspar. The sensitivity changes of BTL and far-red TL in albite gains were investigated by applying thermal treatments in oxidative or reductive condition at various temperatures. Annealed grain samples were stored for seven months and measured TL signal. As a result, BTL sensitivity from oxidative annealed samples decreased during the stored period, while far-red TL sensitivity did not change. Thus, it is suggested that far-red TL will be useful for dating of archaeological materials in which a lot of feldspar constituents are contained.

#### **2P41 : Comparison of retrospective doses by luminescence measurements using quartz and feldspar grain in the atomic bomb-suffered roof tiles (Hiroshima and Nagasaki)**

Nomura, S., <sup>a</sup> Hashimoto, T. <sup>b</sup> (<sup>a</sup> Graduate School of Science and Technology, Niigata Univ., <sup>b</sup> Faculty of Science, Niigata Univ.)

TL measurements has been used for dating of archaeological samples. It will be also useful for retrospective dosimetry. The retrospective doses from quartz and feldspar grains extracted from atomic bomb-suffered roof tiles collected at Hiroshima and Nagasaki, were evaluated by luminescence measurements using SAR protocol. In the case of quartz grains extracted from roof tile in Hiroshima, the retrospective dose by RTL measurements from quartz was estimated to be about 50Gy in good agreement with theoretical results. However, the dose evaluated from Far-red TL of feldspar grains was always lower rather than about 50Gy from RTL of quartz fraction. From these results, it was confirmed that the RTL source in quartz grains possesses preferably stable nature since RTL-source production at atomic-bomb explosion 59 years ago.

#### **2P42 : Luminescence dating of quartz and feldspar grains**

#### **extracted from pieces of Shin-Yakushiji temple roof-tile**

Nakata, Y., <sup>a</sup> Iba, T., <sup>b</sup> Hashimoto, T. <sup>b</sup> (<sup>a</sup>Graduate School of Science and Technology, Niigata Univ., <sup>b</sup>Faculty of Science, Niigata Univ.)

Luminescence technique has been used for dating archaeological samples. In this experiment, the quartz and feldspar grains were extracted from some parts of Shin-Yakushiji temple roof-tile. Accumulated doses were estimated from RTL and BTL measurements of quartz fractions and far-red TL, BTL and IRSL measurements of feldspar aliquots. On the other hand, annual dose was derived from  $\gamma$ -ray spectrometry under dose distribution estimated under consideration of overlapping patterns of roof tiles. Finally, the TL/IRSL ages were obtained by dividing accumulated doses with annual doses. These accumulated doses were also compared among each parts, resulting in the evaluation of lower dose from BTL and IRSL(feldspars) in comparison with RTL evaluate(quartz grains). As a result, RTL age was in good agreement with the predicted age elapsed since the temple building. These results implied that the RTL method for burnt sample gave the evaluation of the equivalent dose values rather than the other method, suggesting the existence of anomalous fading of feldspar.

#### **2P43 : Development of a radon suppression air monitor using time interval analysis (1)**

##### **- Performance test of advanced measurement system -**

Sanada, Y., Nohara, N., Uezu, Y. (JNC Tokai), Hashimoto, T. (Niigata Univ.)

A delayed coincidence method, time-interval analysis (TIA), has been applied to  $\alpha$ - $\beta$  decay events with the microsecond time scale, to detect selectively a correlated decay-event such as  $^{214}\text{Bi} \rightarrow ^{214}\text{Po}$ ( $T_{1/2}=164\mu\text{s}$ ). A radon suppression air monitor has been devised on the basis of application of a TIA-technique. The performance test of advanced TIA-system was carried out using a pulse generator and the circular radioactive-references. As a result, the present measuring system has proven to give  $38\mu\text{s}$  of a dead time. The final TIA detection efficiency of correlated events has been evaluated to be 5%. On the basis of these results, a preferable measurement system has been considered to decrease  $<10\mu\text{s}$  of dead time in addition to furthermore-enhanced detection efficiency of correlated events. For this purpose, the utilization of two Si-detectors, in which sampling filter is inserted has been confirmed to improve the TIA detection efficiency.

#### **3A01 : Correlation between radiation-induced luminescence properties and impurities in growth-parts of synthetic quartz**

Tajika, Y., <sup>a</sup> Yonezawa, Y., <sup>b</sup> Hashimoto, T. <sup>b</sup> (<sup>a</sup>Graduate School of Science

and Technology, Niigata University, <sup>b</sup>Faculty of Science, Niigata University)

After irradiation with ionizing-radiation, some insulating white minerals, such as quartz and feldspar, exhibit both thermoluminescence (TL) and optically stimulated luminescence (OSL), when heated or stimulated with light, respectively. In this work, some synthetic quartz slices, which were grown in different Al-contents in fused solution, were utilized. First of all, slice samples were distinguished from color center image (CCI) and thermoluminescence color image (TLCI) after  $\gamma$ -ray irradiation. Subsequently, four parts (+X, -X, S, Z part) were compared from aspects of TL, Al contents (ICP-MS), OH impurities (IR spectrometry) and ESR measurement. TL intensities made maximum at about 10 ppm Al content. TL intensities also decreased beyond 10 ppm. Li-dependent OH absorption increased rapidly when Al contents reached about 30 ppm. It was considered that Li-dependent OH must produce of radiolysis-hydrogen radicals, which result with decrease luminescence center.

### **3A02 : Dependence of radioluminescence behavior on thermoluminescence properties from natural quartz samples**

Shimizu, N.<sup>1</sup>, Takeuchi, T.<sup>2</sup>, Hashimoto, T.<sup>2</sup>(<sup>1</sup>Graduate School of Science and Technology, Niigata University, <sup>2</sup>Faculty of Science, Niigata University)

When the insulating white minerals, which have been exposed to ionizing radiation, was heated, light emission should occurred as so-called thermoluminescence (TL). These phenomena have been utilized to radiation-dosimetry, dating of archaeological matters and so on. Nowadays, the usefulness of red-TL (RTL)-dating techniques to burnt archaeological-materials has been widely recognized. To approach TL emission mechanism, radioluminescence (RL) measurement was carried out for differently originating quartz samples. RL phenomenon can be observed during the X-ray irradiation. RL behavior was clearly dependent on the irradiation time and kinds of quartz origins. In blue-RL (BRL), the intensities of quartz samples, which exhibit blue-TL (BTL), tend to decay down, whereas RTL-quartz grains showed growing trends. These changes were considered to relate to TL property. So, TL measurements were compared in two temperature ranges, low-temperature TL (-196~50 °C) and high-temperature TL (50~450 °C). Consequently, a certain correlation was found between RL growth and decay behavior and TL-properties.

### **3A03 : Luminescence properties from natural quartz samples**

Fujita, H., <sup>a</sup> Hashimoto, T.<sup>b</sup> (<sup>a</sup>JNC, <sup>b</sup>Niigata Univ.)

Any radioluminescence (RL) phenomena should be observed from many insulating minerals including quartz during the radiation-irradiation. The RL attracts much attention for the purpose of both the alternative dosimetry and the elucidation of luminescence mechanism. In this study, a RL detection equipment was developed to perform the measurement of RL emission wavelength, followed by a RL-behavior change of quartz samples during irradiation. It is noteworthy that the RL spectrum consists of two RL emission regions assigned to emission peaks at 400 (violet) and 630nm (red-colored range). The RL intensity ratios at 400nm and at 630nm wavelengths were found to depend on the places collected quartz samples, probably owing to their provenance. Concerning temperature-changes of samples, the RL behavior indicates evident differences dependent on the exposure times; the Red-RL (R-RL) at 380 °C tended to a faster saturating tendency in comparison with the R-RL at room temperature. Thermal quenching effect on RL was also observed, in which the higher sample temperature causes the lower RL intensities.

### **3A04 : Tritium and ion concentrations in rain**

Toyoshima, T., <sup>a</sup> Momoshima, N., <sup>b</sup> Takahashi, M.<sup>b</sup> (<sup>a</sup>Grad. Sch. Sci. Tech., Kumamoto Univ., <sup>b</sup>Fac. Sci., Kumamoto Univ.)

Tritium and ion concentrations in rain have measured at Kumamoto, Japan from 2001. The purpose of the study is to make clear environmental tritium behavior. Tritium in rain was enriched by electrolysis. 50ml of the enriched rain sample was mixed with 50ml of scintillation cocktail in polyethylene vial, and measured with a low back-ground liquid-scintillation counter. Hydrogen and major ion concentrations were measured with a pH meter and by ion chromatography. The change in tritium concentration observed for these 7 years was speculated to be occurred in relation to the solar activity change. Tritium concentration showed a positive correlation with non-sea-salt ions, indicating a possible long range transport of non-sea-salt materials as well as tritium from China to Japan. This suggests a usefulness of tritium as geographical tracer.

### **3A05 : Time efficiency of tritium measurement in the environmental water by electrolysis enrichment 2**

Sakuma, Y., Yamanishi, H. (National Institute for Fusion Science), Iida, T. (Graduate School of Engineering, Nagoya Univ.), Ogata, Y. (School of Health Science, Nagoya Univ.), Tsuji, N. (Japan Air-conditioning Service Co & Ltd.), Kakiuchi, M. (Fac. of Science, Gakushuin Univ.), Satake, H. (Fac. of Science, Toyama Univ.), Torikai, Y. (Hydrogen Isotope Research Center, Toyama Univ.)

Now tritium concentration in the environmental water samples is very low in Japan, and the electrolysis enrichment is necessary.

However, the measuring procedure with the electrolysis enrichment was very complicated, but it did not give enough accurate results compared with the efforts. We have developed a new method which is able to measure more efficient and more accurate than the conventional method. Using this new method, several measurements were carried out, collecting samples from 7 sampling points every month or every three month during the year of 2003. The results were as follows; the concentrations of tap water samples, rain water and spring water were from 0.1Bq/kg to 0.6 Bq/kg and the concentrations of water vapor in the air at Toki were from 0.5Bq/kg to 1.0Bq/kg.

### **3A06 : Study on transport behavior of particulate organic carbon-14 in river waters from the Tokachi River**

Nagao, S. (Hokkaido Univ.), Aramaki, T. (NIES), Usui, T., Irino, T., Minagawa, M. (Hokkaido Univ.) , Ueno, T., and Matsunaga, T. (JAERI)

Particulate organic matter (POM) in river water is one of carbon materials transported from land to ocean. The study on the behavior and source of POM is important to understand modern carbon cycle. In this study, we present data related to variations of stable and radioactive carbon ratios of temporal series of suspended particulate organic matter from the Tokachi River in Japan. Field experiments were conducted 4 times at a station of the downstream Tokachi River. Approximately 100 l of the water samples were dewatered by use of a single-bowl continuous-flow centrifuge. Radiocarbon and  $\delta^{13}\text{C}$  analyses were performed at the AMS facility of the JAERI-MEL. The  $\Delta^{14}\text{C}$  values (-245‰ and -206‰) of POM collected in April and May were older than those (-160‰ and -101‰) in June and August in 2003. The  $\delta^{13}\text{C}$  values and C/N ratio were also different from spring and summer. These results indicate that the  $\delta^{13}\text{C}$  and  $\Delta^{14}\text{C}$  values of POM reflect the variations of river and watershed environments.

### **3A07 : Measurement of technetium-99 in seaweed samples using rhenium as a tracer**

Tagami, K., Uchida, S. (Natl. Inst. Radiat. Sci.), Mas, J.L. (Huelva Uni.)

Analysis data on  $^{99}\text{Tc}$  in environmental samples should give useful information for predicting the nuclide behavior in the environment. For the determination of  $^{99}\text{Tc}$ , a chemical separation is required due to its low concentration, and therefore the use of a chemical yield tracer is necessary. Rhenium can be used for this purpose because Tc and Re have similar chemical behavior. The application of Re can avoid the use of radioactive isotopes, especially at places where these radioisotopes are strictly forbidden. In this study, Tc recovery was estimated throughout the Re recovery calculation by the isotope dilution technique coupled with ICP-MS in order to measure  $^{99}\text{Tc}$  in seaweed samples. For

chemical separation, a chromatographic resin is used. Interfering elements are removed using a resin washing step carefully designed to avoid any element fractionation between Re and Tc. The average recoveries of  $^{95m}\text{Tc}$  and Re were 93±6 and 95±7%, respectively, within the uncertainty intervals for each other. The results show the possibility of applying Re chemical recoveries to calculate the  $^{99}\text{Tc}$  concentrations without any systematic errors.

### **3A08 : Rapid analytical procedure of plutonium isotopes in soil samples**

Ohtsuka, Y.<sup>1</sup>, Kimura, J.<sup>2</sup>, Nishimura, K.<sup>2</sup>, Takaku, Y.<sup>1</sup>, Hisamatsu, S.<sup>1</sup>, Inaba, J.<sup>1</sup> (<sup>1</sup>Inst. Environ. Sci., <sup>2</sup>Tohoku Nuclear)

A large amount of Pu will be handled in atomic energy industries in Japan. Since most of Pu isotopes emits  $\alpha$ -ray and have long half-lives, it is important to establish a rapid analytical method preparing for accidental Pu release. We developed a rapid analytical method for Pu in soil samples completing within 1 hour. A microwave bead sampler was adapted for alkali fusion of soil sample in this study. After Pu was separated with chelating resin, it was further purified and then determined by on-line column/ID-ICP-MS method. Time required for sample treatment and the determination of Pu was within 1 hr as total, and it showed that this method is very rapid for analysis of Pu in soil samples. Typical lower detection limits were 20 mBq kg<sup>-1</sup> of  $^{239}\text{Pu}$  and 40 mBq kg<sup>-1</sup> of  $^{240}\text{Pu}$ . Results of Pu determination in international certified material were also good.

### **3A09 : Continuous observation of $^{228}\text{Ra}/^{226}\text{Ra}$ activity ratio in river water**

Ohata, T., Sato, J. (Meiji Univ.)

$^{228}\text{Ra}$  and  $^{226}\text{Ra}$  in river water were collected with Mn-impregnated acrylic fiber to observe the contribution of precipitation to the  $^{228}\text{Ra}/^{226}\text{Ra}$  activity ratio. The observation was carried out continuously for the period from May 16 to 28, 2004. The activity ratio decreased with rain fall and recovered afterward.

### **3A10 : A study on the migration of REE and U via groundwater in the Tono uranium deposit by REE patterns**

Takahashi, Y.<sup>1</sup>, Yoshida, H.<sup>2</sup>, Sato, N.<sup>3</sup>, Hama, K.<sup>4</sup>, Shimizu, H.<sup>1</sup> (<sup>1</sup>Dep. of Earth and Planetary Systems Sci., Graduate School of Sci., Hiroshima Univ., <sup>2</sup>Nagoya University Museum, <sup>3</sup>Department of Earth Sci., Kumamoto Univ., <sup>4</sup>Japan Nuclear Cycle Development Institute)

Abundances of rare earth elements plus Y (REE) were determined for granitic rocks, Tertiary sedimentary rocks, and related groundwater in the Tono area, central Japan. Tetrad effects, concave curves in REE

patterns, were found for these rocks and groundwater samples. It should be noted that conjugate M- and W- types of tetrad effects were simultaneously observed in these specimens which constitute the water-rock system; the granitic rocks show the M-type tetrad effects while the groundwater and the sedimentary rocks exhibit the W-type tetrad effects. Non-chondritic Y/Ho ratios were found especially in the groundwater; Y/Ho ratios showed larger values than the chondritic value for the samples showing W-type tetrad effects, and vice versa.. These results suggest that REE, and possibly U, in the sedimentary rocks were transported by the groundwater from the granitic rocks in the Tono area.

### **3A11 : Interaction of U(VI) with bacteria**

Ohnuki T.,<sup>a</sup> Yoshida T.,<sup>a</sup> Ozaki T.,<sup>a</sup> Francis A.J.<sup>b</sup> (<sup>a</sup> JAERI, <sup>b</sup>BNL)

Accumulation experiments of U(VI) with bacteria of *Bacillus subtilis* and *Saccharomyces cerevisiae* were carried out. At pH 4 most of U(VI) was adsorbed on the cells surface of *B. subtilis*. On the contrary, uranyl-phosphate containing precipitates were occurred on the cells of *S. cerevisiae* after the exposure to  $4 \times 10^{-4}$  M U(VI) solution. SEM, TEM, and VIS spectroscopy analyses showed that the precipitate was H-autunite.

### **3B01 : Measurement of Hyperfine Field in Biomolecule by Perturbed Angular Correlation of $\gamma$ -rays**

Hashimoto, T.,<sup>1</sup> Yokoyama, A.,<sup>1</sup> Kataoka, K.,<sup>1</sup> Takata, M.,<sup>1</sup> Kikunaga, H.,<sup>1</sup> Kinoshita, N.,<sup>1</sup> Murakami, Y.,<sup>2</sup> Takamiya, K.,<sup>2</sup> Ohkubo, Y.<sup>2</sup> (<sup>1</sup>Graduate School of Natural Sci. and Tech., Kanazawa Univ., <sup>2</sup>Res. Reactor Inst., Kyoto Univ.)

Perturbed angular correlation of  $\gamma$ -rays (PAC) is a useful method to investigate a hyperfine field in a molecule based on nuclear electric quadrupole interaction. Structure and Function are main subjects of research for proteins. Proteins have biological functions in liquid state. X-ray structure analysis is a popular technique used to analyze the structure of crystallized protein. In this study, taking advantage of the PAC method, the structure of metal site of Mavicyanin, which is a protein molecule with a site of copper, was investigated by using time-differential PAC of  $\gamma$ -rays of  $^{117}\text{Cd}$ . The time dependence of coincident counts of the 90-344 keV cascade  $\gamma$  rays was taken using a measurement system consisting of standard fast-slow electronic modules and four BaF<sub>2</sub> scintillation detectors. It was found that Mavicyanin has only one site for a Cd ion and electric field gradient at the metal position was determined to be  $2.1 \times 10^{22} \text{ V} \cdot \text{m}^{-2}$  for pH 7.5.

### **3B02 : Influence of gamma-ray irradiate on chemical structure of polycrystalline diamond**

Nakahata.T.,<sup>a</sup> Kimura.H.,<sup>a</sup> Oyadzu.M.,<sup>a</sup> Sakamoto.K.,<sup>b</sup> Takahashi.K.,<sup>b</sup> Okada.M.,<sup>c</sup> and Okuno.K.<sup>a</sup> (<sup>a</sup>Radiochemical Res. Lab., Fac. of Sci., Shizuoka Univ., <sup>b</sup>Naka Fusion Res. Establishment, Japan Atomic Energy Res. Institute, <sup>c</sup>Res. Reactor Inst., Kyoto Univ.)

Polycrystalline diamond is a promising candidate for torus window, which is a part of the RF (Radio Frequency) heating system, due to its low dielectric loss and high thermal conductivity. The torus window is exposed with several radiations and high-energy particles produced in fusion reactors. Therefore, their irradiation effects, especially  $\gamma$ -ray irradiation effects, on the diamond characteristics should be elucidated.

The  $\gamma$ -ray irradiation was carried out using  $^{60}\text{Co}$   $\gamma$ -ray source with a dose rate of  $17.1 \text{ Gy h}^{-1}$  for 784 h. Thereafter, the X-ray Photoelectron Spectroscopy (XPS) analysis was performed to investigate the change of diamond structure. It was indicated from the C1s XPS spectra that diamond without  $\gamma$ -ray irradiation had three chemical bonding states (C-C, C-O-C, C=O). For the irradiated diamond, however, only the C-C peak energy was shifted toward lower energy side with increasing the absorbed dose up to 7 kGy, and then kept almost constant. This could be attributed to the dissociation of C-C bond by  $\gamma$ -ray.

### **3B03 : Construction and Mössbauer spectroscopic study of a variety of assembled complexes bridged by ligand having anti-gauche isomer**

Morita, T.,<sup>a</sup> Nakashima, S.,<sup>b</sup> Yamada, K.<sup>a</sup> (<sup>a</sup>Fac. of Sci., Hiroshima Univ., <sup>b</sup>N-BARD, Hiroshima Univ.)

The 1,2-bis(4-pyridyl)ethane complex has a variety of assembled structures depending on anti-gauche isomer. The relation between assembled structure and the electronic state of iron atom was investigated by using the inclusion phenomena and the change of anion from NCS<sup>-</sup> to NCO<sup>-</sup>. X-ray structural analyses revealed the inclusion of biphenyl, 2-nitrobiphenyl, and diphenylmethane into the assembled complexes.  $^{57}\text{Fe}$  Mössbauer spectroscopy suggested the spin-crossover phenomena in the present inclusion complexes. The color also changed by cooling the sample because of the spin change.

### **3B04 : Constructions and physical properties of functional spin transition iron(II) compounds**

Hayami, S.,<sup>a</sup> Miyazaki, S.,<sup>a</sup> Shigeyoshi, Y.,<sup>a</sup> Ogawa, Y.,<sup>b</sup> Kawamata, J.,<sup>c</sup> Kawajiri, R.,<sup>d</sup> Mitani, T.,<sup>d</sup> Maeda, Y.<sup>a</sup> (<sup>a</sup>Kyushu Univ., <sup>b</sup>Kumamoto Univ., <sup>c</sup>Yamaguchi Univ., <sup>d</sup>JAIST)

A number of spin-crossover iron(II) compounds have been studied. They are important in the development of electronic devices such as molecular switches. Here, we synthesized the spin-crossover iron(II) compound  $[\text{Fe}(\text{R})_2(\text{NCS})_2]$  (I) and iron(III) compound

$\text{Na}[\text{Fe}(\text{C16-salen})(\text{CN})_2]$  (**2**). The iron(II) compound **1** has exhibited photo-induced spin transition (LIESST) effect. The ligand R in compound **1** has an asymmetric carbon atom, and the compound **1** is a chiral molecule (R form). Generally, chiral molecules exhibit the second-order non-linear optical (SONLO) response. The NLO response is also dependent on the electronic configuration of the metal center. The spin-crossover compounds exhibited spin transition between a paired and an unpaired electronic configurations can switch the SONLO response. The compound **2** with long alkyl chains has also exhibited spin-crossover behavior. The ligand C16-salen with elongated substituents were employed to provide the liquid crystal properties of the compound **2**. LB film consisting of the compound **2** was prepared, and characterized by SONLO (SHG) measurements.

### 3B05 : The dynamics of the $[\text{FeN}_6]$ core in $[\text{Fe}(2\text{-pic})_3]\text{Cl}_2\text{EtOH}$ studied by NRIS

Juhasz, G.<sup>1</sup> Seto, M.<sup>2</sup> Yoda, Y.<sup>3</sup> Hayami, S.<sup>1</sup> Maeda, Y.<sup>1</sup> (<sup>1</sup>Kyushu Univ., <sup>2</sup>Kyoto Univ., <sup>3</sup>JASRI)

Compounds that can show light-induced phases have always drawn much attention.  $[\text{Fe}(2\text{-pic})_3]\text{Cl}_2\text{EtOH}$  (1, 2-pic: 2-picolyamine) is well-known example of them. In order to study the dynamics of the iron-ligand vibrations in 1,  $^{57}\text{Fe}$  Nuclear Resonant Inelastic Scattering (NRIS) measurements were carried out at Spring-8, BL09XU beamline, with a resolution of  $20 \text{ cm}^{-1}$ . The light-induced HS phase as well as the HS-LS transition was investigated. Indicating a distorted geometry, a considerable splitting of  $T_{1u}$  bond-streching modes can be observed in low-spin as well as the high-spin states. The distortion of the geometry and the splitting of these lines were confirmed by DFT calculations. In contrast with the IR/Raman measurements, no significant difference was found comparing the light-induced and the thermally induced HS state. Our result suggests that the distortion in the light-induced HS phase, observed by IR/Raman methods, has only a minor effect on the dynamics of the  $[\text{FeN}_6]$  core. The novel technique NRIS provides unique information on this compound and deeper insight to the LIESST-effect.

### 3B06 : Mössbauer spectra of the dinuclear iron complexes with the bridging chloranilic acid ligand

Matsuoka,N.<sup>a</sup> Fujii,S.<sup>a</sup> Sakai,H.<sup>a</sup> Nasu,S.<sup>b</sup> (<sup>a</sup>Fac.of Sci. and Eng., Konan Univ., <sup>b</sup>Grad.school of Eng.Sci.Osaka Univ.)

The dinuclear iron complex of formula  $[\text{Fe}_2(\text{tren})_2(\text{CA})](\text{BPh}_4)_2$  {CA= chloranilic acid, tren = tris(2-aminoethyl) amine} has been prepared and characterized from Magnetic susceptibility, Mössbauer spectroscopy, and X-ray diffraction. In the magnetic susceptibility measurements,  $\chi_M T$  product of this complex ( $\chi_M$  being the molar

magnetic susceptibility and T the temperature) is observed to be  $7.18 \text{ cm}^3 \text{ mol}^{-1} \text{ K}$  at 300 K, which corresponds to an effective magnetic moment  $\mu_{\text{eff}} = 7.59 \mu_B$ . This value lies in the range expected for an  $\text{Fe}^{2+}$  dinuclear complex including two noncoupled or weakly coupled high spin metal ions. The  $\mu_{\text{eff}}$  at 300K decreases gradually down to  $\sim 20$  K whereupon the  $\mu_{\text{eff}}$  value decreases more rapidly with decreasing temperature down to  $4.02 \mu_B$  at 5K. The behavior is characteristic of an antiferromagnetic exchange interaction. The Mössbauer spectra of this complex indicate the typical value of high spin state  $\text{Fe}^{2+}$  (I.S.=1.06 mm/s, Q.S.=2.70 mm/s at 80K), consistent with the result of magnetic susceptibility.

### 3B07 : Mössbauer spectra of mixed ligands iron complexes with dihydroxybenzoquinone derivatives

Doiuchi, T., Fujii, S., Sakai, H. (Fac.of Sci. and Eng.,Konan Univ.)

Mixed ligands-iron(II) complexes with chloranilic acid (CA) and dihydroxybenzoquinone (DHBQ) were prepared and characterized by Mössbauer spectroscopy, IR spectra, and the powder X-ray diffraction(XRD). It is confirmed that the CA- and DHBQ-iron(II) complexes consist of a zigzag and a straight chain structure, respectively. Mössbauer spectra and XRD pattern of mixed ligands-iron(II) complexes (the CA content is larger than the DHBQ) are similar to those of the pure CA-iron(II) complex, suggesting the zigzag chain structure with two cis water molecules. On the other hand, in the case of large DHBQ content the DHBQ-type complex, which is the straight chain structure with two trans water molecules, exist in the precipitate in addition to the CA-type complex.

### 3B08 : Mössbauer spectroscopic studies of $[\text{M(L)}]-[\text{Fe}(\text{CN})_6]$ type complexes ( $\text{M} = \text{Cu}, \text{Zn}$ )

Suzuki, N., Katada, M. (Graduate School of Sci. Tokyo Metropolitan Univ.)

Eleven complexes of the type  $[\text{M(L)}]-[\text{Fe}(\text{CN})_6]$  ( $\text{M} = \text{Cu}, \text{Zn}$ ) have been prepared and characterized by XRD, TG-DTA and Mössbauer spectroscopy. Mössbauer parameters, isomer shift and quadrupole splitting suggested that iron ions in many complexes prepared was Fe (III) low spin state. However, a typical single peak was observed in  $[\text{Zn}(\text{dien})_2][\text{Fe}(\text{CN})_6] \cdot 3\text{H}_2\text{O}$ ,  $[\text{Cu}(\text{dien})_2][\text{Fe}(\text{CN})_6] \cdot 4.5\text{H}_2\text{O}$  and  $[\text{Cu}(\text{dien})_2][\text{Fe}(\text{CN})_6] \cdot 4\text{H}_2\text{O}$  indicating Fe(II) low spin state. Two doublet peaks was found in  $[\text{Cu}(4,4\text{-bpy})_3][\text{Fe}(\text{CN})_6] \cdot 3\text{H}_2\text{O}$ . IR spectra showed some of these complexes consist of a polymer structure. These results were supported by Mössbauer spectroscopy.

### 3B09 : $^{57}\text{Fe}$ Mössbauer spectroscopy of Jarosites and related minerals

Takeda, M.<sup>a</sup> Iiyama, T.<sup>a</sup> Sakai, H.<sup>b</sup> Nomura, K.<sup>c</sup> Takahashi, M.<sup>a</sup> (<sup>a</sup>Fac. of Sci., Toho Univ., <sup>b</sup>Professor Emeritus of Okayama Univ., <sup>c</sup>Grad. School of Eng., Univ. of Tokyo)

NASA reported in March 2004 that Mars-Exploration-Rovers Opportunity found the iron sulfate mineral, Jarosites,  $MFe_3(OH)_6(SO_4)_2$  ( $M = K, Na, H_2O$ ) in Meridiani Planum on Mars in fairly large area via  $^{57}\text{Fe}$  Mössbauer spectroscopy. This proves the existence of water in past on Mars. However any value of their Mössbauer parameters are not yet published. This motivated us to carry out Mössbauer spectroscopic study on Jarosites produced on Earth and related sulfate minerals on Earth. We found that the spectrum of Jarosite,  $KFe_3(OH)_6(SO_4)_2$  is completely different from those of anhydrous sulfate, Mikasaite,  $(Fe,Al)_2(SO_4)_3$ , and Yavapaiite,  $KFe(SO_4)_2$ . Thus it is concluded that the spectra of "Jarosite" on Mars can not be explained as due to Mikasaite and Yavapaiite. It is interesting to find that the isomer shifts of  $0.47 \text{ mm s}^{-1}$  for Mikasaite and Yavapaiite are significantly larger than the values of  $0.38 \text{ mm s}^{-1}$  for Jarosite.

### **3B10 : $^{57}\text{Fe}$ Moessbauer spectroscopic study on chemical states of iron in the Antarctic Ocean sediment**

Shozugawa, K.<sup>a</sup> Matsuo, M.<sup>a</sup> Kuno, A.<sup>a</sup> and Miura, H.<sup>b</sup> (<sup>a</sup>Graduate School of Arts and Sciences, The University of Tokyo, <sup>b</sup>National Institute of Polar Research)

The iron species contained in the Antarctic Ocean sediments may have recorded past fluctuation of the ocean environment.  $^{57}\text{Fe}$  Moessbauer spectroscopy has been applied to the sediments to investigate the vertical distribution of iron species. The Moessbauer spectra consisted of three doublets ascribable to one paramagnetic  $\text{Fe}^{2+}$  and two paramagnetic  $\text{Fe}^{3+}$ . The  $\text{Fe}^{2+}$  doublet and one of  $\text{Fe}^{3+}$  doublets were commonly found in the ocean sediments, and attributed to iron in silicate minerals and clay minerals. However, it is noticeable that another  $\text{Fe}^{3+}$  doublet had different Moessbauer parameters from those of clay minerals. The relative peak area of this doublet was found to increase from the last glacial period to the present day. We are now examining the possibility that this component may have some relationships with the organism abundance in the paleoceanography.

### **3B11 : Mössbauer spectra of cathode material for lithium ion battery**

Nishida, T.<sup>a</sup> Tokunaga, M.<sup>a</sup> Yamamoto, T.<sup>b</sup> Okada, S.<sup>b</sup> Yamasaki, J.<sup>b</sup> (<sup>a</sup>School Human.-Orient. Sci. Eng., Kinki Univ., <sup>b</sup>Inst. Materi. Chem. Eng., Kyushu Univ.)

Alfa- $\text{FePO}_4$ (P321) for the cathode material of new lithium ion battery was prepared by heating a mixture of iron powder,  $\text{P}_2\text{O}_5$ , and

water at  $100\text{-}650^\circ\text{C}$ . Mössbauer spectra of alfa- $\text{FePO}_4$  shows a complete reduction of  $\text{Fe(III)}$  to  $\text{Fe(II)}$  after full-discharge of the battery. The reduced  $\text{Fe(II)}$  is completely oxidized to  $\text{Fe(III)}$  after full-charge of the battery. Redox of iron is quantitatively observed by discharge and charge of the battery.

